

Consistent Excesses in the LHC Electroweak SUSY Searches: GUT-based Singlino/Higgsino Interpretation in the NMSSM

EMANUELE BAGNASCHI^{1*}, MANIMALA CHAKRABORTI^{2†}, SVEN HEINEMEYER^{3‡}
AND IPSITA SAHA^{4§}

¹*INFN, Laboratori Nazionali di Frascati, Via E. Fermi 40, 00044 Frascati (RM), Italy*

²*School of Physics and Astronomy, University of Southampton, Southampton, SO17 1BJ, United Kingdom (former address)*

³*Instituto de Física Teórica (UAM/CSIC), Universidad Autónoma de Madrid, Cantoblanco, 28049, Madrid, Spain*

⁴*Department of Physics, Indian Institute of Technology Madras, Chennai 600036, India*

Abstract

The search for signatures of supersymmetric models remains one of the main items on the BSM search program at the LHC, with EW SUSY partners still allowed with masses as low as a few hundred GeV. Over the last years, searches for the “golden channel”, $pp \rightarrow \tilde{\chi}_2^0 \tilde{\chi}_1^\pm \rightarrow \tilde{\chi}_1^0 Z^{(*)} \tilde{\chi}_1^\pm W^{\pm(*)}$ show consistent excesses between ATLAS and CMS in the 2 soft-lepton and 3 soft-lepton plus \cancel{E}_T searches, assuming $m_{\tilde{\chi}_2^0} \approx m_{\tilde{\chi}_1^\pm} \gtrsim 200$ GeV and $\Delta m_{21} := m_{\tilde{\chi}_2^0} - m_{\tilde{\chi}_1^0} \approx 20$ GeV. We interpret these excesses in the framework of the Next-to-Minimal Supersymmetric Standard Model (NMSSM). We assume a singlino dominated lightest neutralino, $\tilde{\chi}_1^0$, as a Dark Matter (DM) candidate. The second and third lightest neutralinos, $\tilde{\chi}_{2,3}^0$ are higgsino like, with the higgsino mixing parameter μ being smaller than the soft SUSY-breaking bino and wino masses, M_1 and M_2 . We furthermore assume the approximate GUT relations $M_1 \sim M_2/2 \sim M_3/6$, with the implication for our scenario of a gluino mass $m_{\tilde{g}} \sim M_3 \gtrsim 3$ TeV. Scalar masses are assumed to be heavy and do not play a role in our analysis. We find that this scenario is in agreement with all relevant experimental constraints, comprising the LHC searches for SUSY particles and additional Higgs bosons, the LHC Higgs-boson rate measurements, the DM direct detection limits and the upper limit on the DM relic density. We demonstrate that this scenario gives an excellent description of the observed excesses in the search for 2 and 3 soft-leptons plus \cancel{E}_T , with $m_{\tilde{\chi}_2^0} \sim m_{\tilde{\chi}_3^0} \sim m_{\tilde{\chi}_1^\pm}$ and $\Delta m_{21} \sim 20$ GeV. This constitutes the first explanation of the soft-lepton excesses in a model with GUT relations among the soft SUSY-breaking parameters.

*email: emanuele.angelo.bagnaschi@lnf.infn.it

†email: M.Chakraborti@soton.ac.uk

‡email: Sven.Heinemeyer@cern.ch

§email: ipsita@iitm.ac.in

1 Introduction

The Standard Model (SM) of particle physics remains one of our most successful theories ever, being able to describe with high precision (most of) the wealth of currently available experimental data, covering a large span in energy scales. Yet we know from cosmological and astrophysical observations that physics beyond the SM is required to explain various phenomena, such as the ones interpreted today in terms of Dark Matter (DM). One of the most promising models, among the plethora of theories Beyond the SM (BSM) containing a viable DM candidate, is the Minimal Supersymmetric (SUSY) Standard Model (MSSM) [1–4] (for a recent review, see Ref. [5]). The MSSM features, for each SM field, a superpartner that differs by one-half unit spin. Moreover, supersymmetry requires extending the Higgs sector from one to two Higgs doublets. As a consequence, the physical spectrum of the theory contains five Higgs bosons instead of a single one, as instead happens in the SM. The Higgs sector therefore consists of the light and heavy \mathcal{CP} -even Higgs bosons (h and H), the \mathcal{CP} -odd Higgs boson (A), as well as a pair of charged Higgs bosons (H^\pm). Concerning the electroweak (EW) sector of the MSSM, it contains the SUSY partners of the SM leptons, the scalar leptons (sleptons), as well as the charged (neutral) SUSY partners of the charged (neutral) EW gauge bosons (gauginos) and Higgses (higgsinos). After electroweak symmetry breaking, gauginos and higgsinos mix to form two charginos ($\tilde{\chi}_{1,2}^\pm$) and four neutralinos ($\tilde{\chi}_{1,2,3,4}^0$), the so-called “EWinos”. The searches for the production and decays of the EWinos and sleptons in various final states are one of the primary targets in BSM searches at the LHC.

In the MSSM with conserved R-parity (which we assume throughout the paper), the lightest neutralino, $\tilde{\chi}_1^0$, assumed to be the lightest SUSY particle (LSP), can play the role of a weakly interacting massive particle (WIMP) DM candidate [6, 7]. The masses and mixings of the neutralinos and charginos are governed by two soft SUSY-breaking parameters, the $U(1)$ parameter M_1 , the $SU(2)$ parameter M_2 , as well as the SUSY-conserving Higgs mixing parameter μ . The latter parameter poses a theoretical problem. It is a SUSY-conserving parameter, but its value is not protected by any symmetry. However, experimentally it must be at the scale of the other soft SUSY-breaking parameters. This was dubbed the “ μ -problem” of the MSSM [8].

In order to solve the “ μ -problem”, the extension of the MSSM by a gauge-singlet superfield – the Next-to MSSM (NMSSM) [9, 10] – was introduced [8]. The addition of the singlet superfield, containing a singlet scalar and a singlet fermion (the singlino) enlarges the spectrum of the theory. The neutralino sector of the NMSSM, with the addition of the singlino, contains five neutralinos, $\tilde{\chi}_{1,2,3,4,5}^0$. The Higgs-boson spectrum is extended by one \mathcal{CP} -even and one \mathcal{CP} -odd Higgs-boson, resulting in three \mathcal{CP} -even states (h_1, h_2, h_3), two \mathcal{CP} -odd states (A_1, A_2) and a pair of charged Higgs-bosons (H^\pm). Here we identify the h_1 with the Higgs boson discovered at the LHC with $m_{h_1} \sim 125$ GeV.

In addition to the MSSM parameters, the NMSSM has additional independent parameters related to the singlet superfield. Following the common nomenclature, we choose: $\lambda, \kappa, A_\kappa, A_\lambda$ and the effective parameter μ_{eff} as independent inputs. In the NMSSM, the μ parameter of the MSSM is generated dynamically as $\mu_{\text{eff}} := \lambda v_s$ (where v_s denotes the singlet vev), solving the above mentioned μ problem. From this relation one can determine the value of

v_s as a function of λ and μ_{eff} .

One of the most effective approaches to probe the EW (N)MSSM parameter space, is to search for the lighter EWinos, $\tilde{\chi}_{2,3}^0$ and $\tilde{\chi}_1^\pm$, in final states containing two or three (possibly soft) leptons accompanied by substantial missing transverse energy (\cancel{E}_T) [11–17]. These searches turn out to be particularly challenging in the region of parameter space where the mass difference between the initially produced and the final state EWinos are small [18, 19], making the visible decay products, i.e. the leptons, to be rather soft [20–24]. The mass configuration is commonly referred to as “compressed spectra”. The CMS and ATLAS collaborations are actively searching for the EWinos in this compressed spectra region. Interestingly, over the last years searches for the “golden channel” (focusing for simplicity to the MSSM particle content), $pp \rightarrow \tilde{\chi}_2^0 \tilde{\chi}_1^\pm \rightarrow \tilde{\chi}_1^0 Z^* \tilde{\chi}_1^0 W^{\pm*}$ show consistent excesses between ATLAS and CMS in the 2 soft-lepton and 3 soft-lepton plus missing energy [25, 26]. This also holds for the combined 2/3 soft-leptons plus \cancel{E}_T [27–29] searches assuming $m_{\tilde{\chi}_2^0} \approx m_{\tilde{\chi}_1^\pm}$ for a mass difference of $\Delta m_{21} := m_{\tilde{\chi}_2^0} - m_{\tilde{\chi}_1^\pm} \approx 20$ GeV.¹ Therefore, it seems naturally interesting to identify the underlying parameter configuration of the EW (N)MSSM and the associated properties of the EWinos that can give rise to such excesses at the LHC.

In Ref. [30] within the MSSM three different scenarios were analyzed, classified by the hierarchy and signs of the EWino mass parameters, M_1 , M_2 and μ , while assuming heavy sleptons. These scenarios are named after their DM candidate, i.e. the largest component of the $\tilde{\chi}_1^0$. The mass configuration favored by the experimental excesses in the compressed spectra searches for EWkinos is naturally found in two of these scenarios:

- (i) wino/bino(+) DM with $\tilde{\chi}_1^\pm$ -coannihilation ($M_1 \lesssim M_2 < \mu$), with $M_1 \times \mu > 0$,
- (ii) wino/bino(-) DM with $\tilde{\chi}_1^\pm$ -coannihilation ($|M_1| \lesssim M_2 < \mu$), with $M_1 \times \mu < 0$,
- (iii) higgsino(-) DM ($|\mu| < |M_1|, M_2$), with $M_1 \times \mu < 0$.

In Ref. [30] all relevant experimental constraints were taken into account. The experimental results comprised of the DM relic abundance [31], the DM direct detection (DD) experiments [32] and the direct searches at the LHC [11, 12].² In Ref. [30] it was found that the wino/bino(-) scenario gives the best description of the excesses, followed by wino/bino(+), which tended to slightly lower Δm_{21} . On the other hand, it was concluded that the higgsino(-) scenario cannot yield a sufficiently large Δm_{21} . This was particularly due to the bounds from DD experiments, excluding the range $\Delta m_{21} \gtrsim 10$ GeV, which would, however, be required to describe the soft-lepton excesses.

Other analyses of the soft-lepton excesses interpreted within the (N)MSSM framework can be found in Refs. [39–45]. More in detail, in Refs. [40–42, 44], various MSSM scenarios have been explored in the context of the soft-lepton excesses. While Ref. [41] investigated the

¹In the following we denote as $\Delta m_{ij} := m_i - m_j$, where $i, j = 1, 2, 3$ stands for the three lightest neutralinos, and $i, j = \pm$ for the lightest chargino.

²A wider range of this type of models taking into account these constraints was analyzed previously in Refs. [33–38].

higgsino-like LSP scenario within the MSSM, Refs. [40, 42, 44] examined both the mono-jet and soft-lepton excesses simultaneously for a simplified higgsino-like scenario. Another combination of various experimental searches has recently been published in Ref. [45]. Within the NMSSM framework, Ref. [39] considered a light higgsino-like triplet corresponding to the lightest chargino and next-to-lightest neutralinos, while assuming a singlino-like LSP that is nearly mass-degenerate with the triplet states. This study also imposed an additional constraint requiring a 95 GeV singlet-like Higgs state. In contrast, Ref. [40] assumed a higgsino–singlino mass splitting of 5–20 GeV, where the decay products from the higgsino-to-singlino transition contribute to the observed signal. The aim of that analysis was to identify the best-fit parameter region capable of accommodating both the soft-lepton and mono-jet excesses. This study has also incorporated a recasting of the relevant analysis using the package `HACKANALYSIS 2` [46]. More recently, Ref. [43] performed a comprehensive parameter scan of the NMSSM parameter space, where the soft-lepton excess along with a 95 GeV and a 650 GeV scalar resonance was also discussed.

As noted in Ref. [30], the wino/bino(−) and wino/bino(+) scenarios, while giving a good description of the soft-lepton excesses and complying with the DM experimental constraints, require $|M_1| \sim |M_2|$. Here it is important to note that one of the most compelling arguments in favor of SUSY is the unification of forces at the Grand Unified Theory (GUT) scale [47]. In simple GUT realizations, such as the CMSSM [48], this yields the following mass pattern at the EW scale: $M_1 \sim M_2/2 \sim M_3/6$, where M_3 is the $SU(3)$ soft SUSY-breaking parameter, which coincides with the gluino mass, $M_3 \sim m_{\tilde{g}}$. Searches for colored particles at the LHC have set a limit of $m_{\tilde{g}} \gtrsim 2$ TeV [49, 50], for the relatively light $\tilde{\chi}_1^0$ we are interested in, leading to $|M_1| \gtrsim 350$ GeV, which is too large to yield $m_{\tilde{\chi}_1^0} \lesssim 200$ GeV. Consequently, the MSSM scenarios that can describe the soft-lepton excesses do not follow the GUT-based mass pattern. On the other hand, a GUT-based mass pattern seems to yield too high neutralino and chargino masses, well above 300 GeV.

In this paper we propose a scenario that can describe well the soft-lepton excesses, follows the GUT-based mass patterns and is in agreement with the searches for gluinos: the NMSSM with a singlino dominated LSP, with $200 \text{ GeV} \approx |\mu| < M_1 \sim M_2/2 \sim M_3/6$, and $m_{\tilde{g}} \gtrsim 2$ TeV. This parameter space corresponds to higgsino-like $\tilde{\chi}_{2,3}^0$ and $\tilde{\chi}_1^\pm$. The LHC searches are interpreted as searches for $pp \rightarrow \tilde{\chi}_{2,3}^0 \tilde{\chi}_1^\pm \rightarrow \tilde{\chi}_1^0 Z^* \tilde{\chi}_1^{\pm*} W^{\pm*}$ in the NMSSM, leading to the desired 2 or 3 soft-lepton plus \cancel{E}_T final states. We show that this “singlino/higgsino” scenario can give rise to the ‘correct’ abundance of DM relic density, while agreeing with the latest DD bounds. Concerning the DD limits, the exchange of all \mathcal{CP} -even Higgs bosons can contribute in a significant way, see Ref. [51] for a recent analysis. Consequently, we leave the Higgs-boson sector parameters as free parameters, leading to a variation of the new Higgs-boson mass scales and the properties of the h_1 . We demonstrate that besides the above listed characteristics of the chargino/neutralino sector also the Higgs-boson sector properties are in agreement with the LHC searches for BSM Higgs bosons, as well as with the current LHC Higgs-boson rate measurements. However, the possibility is left open to probe deviations with respect to the SM in the properties of the lightest \mathcal{CP} -even Higgs at ~ 125 GeV, or the existence of new Higgs bosons, at future runs of the (HL-)LHC.

This paper is organized as follows. In Sect. 2 we briefly review the parameters of the

chargino/neutralino and Higgs sectors of NMSSM, fix our notations and define the scenario under investigation. The relevant constraints for this analysis, in particular the excesses in the searches for $\tilde{\chi}_{2,3}^0 \tilde{\chi}_1^\pm$ at the LHC, are briefly summarized in Sect. 3. The scenario we are analyzing, together with our analysis flow is detailed in Sect. 4. In Sect. 5 we present the details of our results as well as the prospects for future DD experiments. The conclusions can be found in Sect. 6.

2 The chargino/neutralino and Higgs sectors of the NMSSM

In this section, we review the chargino/neutralino and the Higgs sectors of the NMSSM, in order to highlight the most important properties of the model, and fix our notation. The scalar quark and lepton sectors are assumed to be heavy and not to play a relevant role in our analysis. Throughout this paper we also assume that all parameters are real, i.e. the absence of \mathcal{CP} -violation.

We consider the Z_3 invariant NMSSM with the superpotential

$$W_{\text{NMSSM}} = \lambda \hat{S} \hat{H}_2 \cdot \hat{H}_1 + \frac{\kappa}{3} \hat{S}^3 + \dots \quad (1)$$

Here the ellipses denote the Yukawa couplings of the Higgs superfields, which are the same as in the MSSM. Denoting the vev of the scalar component of the singlet superfield as $\langle S \rangle = v_s$, see Eq. (7) below, the first term in the superpotential gives rise to the effective μ term,

$$\mu_{\text{eff}} := \lambda v_s. \quad (2)$$

In the remainder of the paper we will omit the subscript $_{\text{eff}}$. We furthermore denote with $\tan \beta$ the ratio of the two vevs of the two Higgs doublets of MSSM, $\tan \beta = v_2/v_1$.

2.1 The chargino/neutralino sector

The NMSSM neutralinos are the linear superpositions of the neutral $SU(2)_L$ and $U(1)_Y$ gauginos, neutral higgsinos and the singlino $\tilde{B}, \tilde{W}^3, \tilde{H}_2^0, \tilde{H}_1^0$ and \tilde{S} , respectively. Their masses and mixings are determined by $U(1)_Y$ and $SU(2)_L$ gaugino masses M_1 and M_2 , the Higgs mixing parameter μ and the singlino mass term. The neutralino mass matrix in the basis $(-i\tilde{B}, -i\tilde{W}^3, \tilde{H}_2^0, \tilde{H}_1^0, \tilde{S})$ is given by

$$M_N = \begin{pmatrix} M_1 & 0 & -M_Z c_\beta s_w & M_Z s_\beta s_w & 0 \\ 0 & M_2 & M_Z c_\beta c_w & -M_Z s_\beta c_w & 0 \\ -M_Z c_\beta s_w & M_Z c_\beta c_w & 0 & -\mu & -\lambda v_2 \\ M_Z s_\beta s_w & -M_Z s_\beta c_w & -\mu & 0 & -\lambda v_1 \\ 0 & 0 & -\lambda v_2 & -\lambda v_1 & 2\kappa v_s \end{pmatrix}, \quad (3)$$

where c_β (s_β) denotes $\cos \beta$ ($\sin \beta$) and $c_w = \sqrt{1 - s_w^2} = M_W/M_Z$ denotes effective weak leptonic mixing angle, and M_W, M_Z are the mass of the W and Z boson, respectively. After diagonalization, the five eigenvalues of the matrix give the five neutralino masses $m_{\tilde{\chi}_1^0} < m_{\tilde{\chi}_2^0} < m_{\tilde{\chi}_3^0} < m_{\tilde{\chi}_4^0} < m_{\tilde{\chi}_5^0}$. The diagonalization matrix is denoted as N , such that

$$N M_N N^T = \text{diag}(m_{\tilde{\chi}_1^0}, m_{\tilde{\chi}_2^0}, m_{\tilde{\chi}_3^0}, m_{\tilde{\chi}_4^0}, m_{\tilde{\chi}_5^0}). \quad (4)$$

As discussed above, the lightest neutralino, $\tilde{\chi}_1^0$ is the LSP and is assumed to give rise to part or the full DM relic density, see Sect. 3 below.

The chargino mass eigenstates, as in the MSSM, are given by the mixing between the charged winos and higgsinos ($\tilde{W}^\pm, \tilde{H}_{2/1}^\pm$) respectively with their mass matrix given by,

$$M_C = \begin{pmatrix} M_2 & \sqrt{2}M_W c_\beta \\ \sqrt{2}M_W s_\beta & \mu \end{pmatrix} \quad (5)$$

Diagonalizing M_C with a bi-unitary transformation, yields the two chargino-mass eigenvalues $m_{\tilde{\chi}_1^\pm} < m_{\tilde{\chi}_2^\pm}$.

Throughout our analysis we neglect \mathcal{CP} -violation and assume μ, M_1, M_2 to be real. From general considerations, even sticking to real parameters, one could choose some (or all) of the mass parameters negative. However, here it is important to note that the results for physical observable are affected only by certain combinations of signs (or, in general, phases). Without loss of generality, it is possible to rotate the phase of M_2 away, i.e. choose (M_2 real and) $M_2 > 0$. This leaves in principle the signs of M_1 and μ free. We choose M_1 to be positive, to allow for the GUT condition $M_1 \sim M_2/2 \sim M_3/6$, leaving the sign of μ free. Consequently, we will explore both combinations, $(M_1 \times \mu) > 0$ and $(M_1 \times \mu) < 0$.

2.2 The Higgs-boson sector

Following Eq. (1) the Higgs potential contains additional terms w.r.t. the MSSM case,

$$V_{\text{NMSSM}} \supset |\lambda(H_1^+ H_2^- - H_1^0 H_2^0) + \kappa S^2|^2 + (\lambda A_\lambda (H_1^+ H_2^- - H_1^0 H_2^0) S + \kappa A_\kappa S^3 + \text{h.c.}), \quad (6)$$

where H_1, H_2 and S denote the scalar parts of their respective superfields. Assuming the following decomposition for the two neutral components of the doublets and the one singlet Higgs fields,

$$H_{i=1,2}^0 = v_i + \frac{1}{\sqrt{2}} (S_i + iP_i), \quad S = v_s + \frac{1}{\sqrt{2}} (S_3 + iP_3), \quad (7)$$

the mass matrix for the \mathcal{CP} -even sector is given by,

$$\begin{aligned}
\mathcal{M}_{\mathcal{CP}\text{-even}} &= \\
&= \begin{pmatrix} \bar{g}^2 v_1^2 - \mu \tan \beta A_\Sigma & (2\lambda^2 - \bar{g}^2) v_1 v_2 + \mu A_\Sigma & 2\lambda \mu v_1 + \lambda v_2 (A_\Sigma + \kappa v_s) \\ (2\lambda^2 - \bar{g}^2) v_1 v_2 + \mu A_\Sigma & \bar{g}^2 v_2^2 - \mu \cot \beta A_\Sigma & 2\lambda \mu v_2 + \lambda v_1 (A_\Sigma + \kappa v_s) \\ 2\lambda \mu v_1 + \lambda v_2 (A_\Sigma + \kappa v_s) & 2\lambda \mu v_2 + \lambda v_1 (A_\Sigma + \kappa v_s) & -\lambda A_\lambda \frac{v_1 v_2}{v_s} + \kappa v_s (A_\kappa + 4\kappa v_s) \end{pmatrix} \quad (8)
\end{aligned}$$

where we have followed the notation of Ref. [52], and defined $A_\Sigma = A_\lambda + \kappa v_s$ and $\bar{g}^2 = (g^2 + g'^2)/2$. Upon diagonalization by an orthogonal matrix R^s , we have three \mathcal{CP} -even mass-ordered eigenstates $h_{1,2,3}$. Note that the tree-level upper bound on the lightest \mathcal{CP} -even mass is higher than in the MSSM and given by:

$$m_{h_1}^2 < m_Z^2 \cos^2(2\beta) + \lambda^2 (v_1^2 + v_2^2) \sin^2(2\beta). \quad (9)$$

The additional term is relevant for values of $\tan \beta \lesssim 10$.

The mass matrix for the \mathcal{CP} -odd sector is given by:

$$\begin{aligned}
\mathcal{M}_{\mathcal{CP}\text{-odd}} &= \\
&= \begin{pmatrix} -\mu \tan \beta A_\Sigma & -\mu A_\Sigma & -\lambda v_2 (A_\Sigma - 3\kappa v_s) \\ -\mu A_\Sigma & -\mu \cot \beta A_\Sigma & -\lambda v_1 (A_\Sigma - 3\kappa v_s) \\ -\lambda v_2 (A_\Sigma - 3\kappa v_s) & -\lambda v_1 (A_\Sigma - 3\kappa v_s) & -4\lambda \kappa v_1 v_2 - \lambda A_\lambda \frac{v_1 v_2}{v_s} - 3\kappa A_\kappa v_s \end{pmatrix}. \quad (10)
\end{aligned}$$

After diagonalization via an orthogonal matrix, we obtain three eigenstates, G^0 , A_1 and A_2 , where the first one is the would-be Goldstone boson that gives mass to the Z , and A_1 and A_2 are two \mathcal{CP} -odd Higgses, again with mass-ordered labeling.

On the top of the neutral Higgses, we have a charged Higgs boson sector with the same structure as in the MSSM. Thus, the physical spectrum of the Higgs sector of the NMSSM contains three \mathcal{CP} -even states (h_1 , h_2 , h_3 , ordered in mass), two \mathcal{CP} -odd states (A_1 , A_2 , ordered in mass) and a pair of charged Higgs-bosons (H^\pm).

We use the code `NMSSMTools` [53–56] as our spectrum generator, which we instruct to compute the Higgs sector masses using the full 1-loop and the 2-loop corrections computed in Ref. [57], and implemented in the code. The following set of parameters is used as input: λ , κ , A_λ , A_κ , μ_{eff} , with v_s obtained from Eq. (2), to define the NMSSM Higgs sector, on top what is already required in the MSSM.

We identify the lightest \mathcal{CP} -even Higgs boson, h_1 , with the Higgs boson discovered at the LHC with $m_{h_1} \sim 125$ GeV. Since the loop corrections involving the top/stop sector are of particular importance for the NMSSM Higgs-boson sector (see Ref. [58] for a review), for the diagonal soft SUSY-breaking parameters in the stop/sbottom sector we have chosen fixed values that are sufficiently large to make it easy to achieve $m_{h_1} \sim 125$ GeV [58], i.e. $M_{Q_3} = M_{U_3} = M_{D_3} = 3$ TeV. Moreover, with this choice the masses of the scalar tops/sbottoms are safely above the LHC limits, and we are not required to implement stop and sbottom searches in our framework.

While in general it is possible to identify also h_2 with the state at ~ 125 GeV and have h_1 as a so far undetected Higgs-boson (see, however, Refs. [39, 59–68] as well as Refs. [69–71] for closely related SUSY models), we leave this possibility for future work.

Following the analysis in Ref. [30], but contrary to our previous analyses [33–38], the heavy \mathcal{CP} -even Higgs bosons can play a relevant role in the (cancellation of the) contributions to the DD cross sections, where all h_1 , h_2 and h_3 exchanges can contribute.

The fact that we treat the Higgs-boson sector parameters as free will require us to check the Higgs sector against experimental constraints from BSM Higgs-boson searches, as well as LHC Higgs-boson rate measurements, as will be discussed below.

3 Experimental constraints

Here we briefly list the experimental constraints that we apply to our data sets. These are a combinations of constraints included in `NMSSMTools`, with others that are handled in our code (i.e. DM constraints, properties of H_{125} and the constraints on the extended scalar sector). As we will describe more in detail in Sect. 4, we use `NMSSMTools` as our spectrum generator, but it also includes the implementation of some of the constraints that we consider in our analysis.

- Vacuum stability constraints:
In the scenario we are interested in studying (see Sec. 4) all the sleptons are relatively heavy, and all the corresponding trilinear couplings set to zero. Thus the scalar potential is not influenced in any relevant way by the slepton sector. In the scalar quark sector, all the soft SUSY-breaking masses are heavy as well. For stop/sbottom sector, we set $A_b = 0$ while we scan over A_t . However, the combination of heavy mass terms with the Higgs mass constraint makes vacuum stability a non-issue, as it was explicitly verified with the constraint on the stability of the effective potential computed by `NMSSMTools`.
- Landau poles:
`NMSSMTools` checks for the presence of Landau poles in the running couplings of the theory up to M_{GUT} .
- DM relic density constraints:
The latest results from the Planck experiment [31] provide the experimental data. The relic density is given by,

$$\Omega_{\text{CDM}}h^2 = 0.120 \pm 0.001, \quad (11)$$

which we use as an upper bound (calculated using the central value with 2σ upper limit),

$$\Omega_{\text{CDM}}h^2 \leq 0.122. \quad (12)$$

The calculation of the relic density in the NMSSM is performed with the code `MicrOMEGAs-6.0` [72–80] as included in `NMSSMTools`.

- DM direct detection (DD) constraints:

We use the latest spin-independent (SI) DM scattering cross-section (σ_{SI}^p) limits from the PandaX-4T [81] experiment that we implement ourselves. These results were the strongest published results at the moment of our data evaluation. Meanwhile, also new LZ results [82] were published, yielding even stronger limits. We will comment on their possible effects (and include them) in future evaluations. Also XENONnT published new results [83], which, however, are weaker than the ones from PandaX-4T. Limits on spin-dependent (SD) scattering cross sections are again implemented using the PandaX-4T results [81], since they were the strongest available, for both SD scattering on protons (SDp) and on neutrons (SDn). As will be shown below, only the limits from SDn will play a role, and only a minor one in comparison with the SI limits. The theoretical predictions are calculated with the code `MicrOMEGAs`, again as included in `NMSSMTools`.

For “underabundant” parameter points (i.e. with $\Omega_{\tilde{\chi}} h^2 \leq 0.118$), the DM scattering cross-section is rescaled by $(\Omega_{\tilde{\chi}} h^2 / 0.118)$. In this way it is taken into account that the $\tilde{\chi}_1^0$ provides only a fraction of the total DM relic density of the universe.

- Indirect DM detection:

Another set of potentially relevant constraints is given by the indirect detection (ID) of DM. We do not, however, impose these constraints on our parameter space because of the well-known large uncertainties associated with astrophysical factors (e.g. the galactic DM density profile, theoretical corrections etc., see Refs. [84–87]). The currently most precise indirect detection limits arise from DM-rich dwarf spheroidal galaxies, where the uncertainties on the cross section limits are found in the range of $\sim 2-3$ [88, 89]. The most severe constraint from the latest analysis in Ref. [88], assuming only one single dominant DM annihilation mode, sets a limit of $m_{\tilde{\chi}_1^0} \gtrsim 100$ GeV, for a generic thermal relic saturating Eq. (11). However, this limit is much weaker than all other experimental constraints (in particular the DD limits described above and the LHC search limits described below) considered in this study.

- Constraints from LHC Higgs-boson rate measurements:

Any viable BSM model has to accommodate a Higgs boson with mass and signal strengths as they were measured at the LHC. For each point in our parameter space we test (see the next section) the compatibility of the lightest \mathcal{CP} -even scalar in the NMSSM, h_1 , with a mass of ~ 125 GeV, with the measurements of signal strengths at the LHC is tested with the code `HiggsSignals v.3` [90–93], which is included in the code `HiggsTools` [93, 94]. The code provides a statistical χ^2 for the h_1 (or any Higgs boson assumed to correspond to the state discovered at the LHC) predictions in comparison to the measurements of the Higgs-boson signal rates and masses from the LHC. We consider acceptable parameter points that do not deviate more than $\Delta\chi^2 := \chi_{h_1}^2 - \chi_{\text{min}}^2 < 6.18$, where the value of $\chi_{\text{min}}^2 \simeq \chi_{\text{SM}}^2 \approx 151$ is determined from our sample and found to be compatible with a SM-like Higgs.

One possible source for large effects beyond the SM are additional contributions in the loop-induced process $h \rightarrow \gamma\gamma$. Here, in particular, a light chargino can yield large corrections. However, this is automatically tested and taken into account via the above detailed approach. Conversely, deviations in $h \rightarrow \gamma\gamma$ may be interesting targets to cross-check the NMSSM explanation of the observed excesses. We will comment more on this in Sec. 5.

- Constraints from direct Higgs-boson searches at the LHC:
The exclusion limits at the 95% C.L. of all relevant BSM Higgs boson searches (including Run 2 data from the LHC are taken into account with the help of the public code `HiggsBounds v.6` [93, 95–99], which is included in the public code `HiggsTools` [93, 94]. For a parameter point in a particular model (the NMSSM in our case), `HiggsBounds` determines on the basis of expected exclusion limits which is the most sensitive channel to test each BSM Higgs boson. In the next step, based on this most sensitive channel, `HiggsBounds` determines whether the point is allowed or not at the 95% CL.
- Constraints from flavor physics:
Flavor constraints can be particularly sensitive to contributions involving charged Higgs bosons [100, 101]. In particular, the decays $B \rightarrow X_s \gamma$ and $B_s \rightarrow \mu^+ \mu^-$ are most relevant. For the scenarios that we are considering, we do not expect large contributions to these observables due to the charged Higgs mass being larger than 1 TeV. We also include other flavor constraints, such as ΔM_d , ΔM_s , $B^+ \rightarrow \tau \nu_\tau$, $\Upsilon(1S) \rightarrow H/A \gamma$, $m_{\eta_b(1S)}$, $\text{BR}(B \rightarrow X_s \mu^+ \mu^-)$, $b \rightarrow d \gamma$, $B_d \rightarrow \mu^+ \mu^-$, $b \rightarrow s \nu \bar{\nu}$ and $K \rightarrow \pi \nu \bar{\nu}$, as implemented in `NMSSMTools`. However, they do not have any relevant impact on our analysis. Moreover, we choose not to consider $(g-2)_\mu$ as anomalous. Given our choice of keeping the slepton sector heavy, SUSY contributions to this observables will be very small and therefore automatically compatible with a SM-like measurement.
- Searches for EWinos at LEP:
The constraints on $m_{\tilde{\chi}_1^\pm}$ and $m_{\tilde{\chi}_1^0}$ (from the measurement of the invisible Z -boson decay width) coming from LEP analyses are implemented via `NMSSMTools`. The constraint on the lightest chargino mass, $m_{\tilde{\chi}_1^\pm} \gtrsim 100$ GeV, lead to a lower limit of $|\mu| \gtrsim 100$ GeV, for our scenario.
- Searches for EWinos at the LHC:
In this analysis we are interested in the $\tilde{\chi}_{2,3}^0 \tilde{\chi}_1^\pm$ pair production searches with decays via $Z^{(*)}$ and $W^{(*)}$ into final states involving 2-3 soft leptons and large \cancel{E}_T . Here it should be kept in mind that the original analyses by ATLAS and CMS were performed in the context of the MSSM, i.e. targeting the process $pp \rightarrow \tilde{\chi}_2^0 \tilde{\chi}_1^\pm \rightarrow \tilde{\chi}_1^0 Z^* \tilde{\chi}_1^\pm W^*$. The relevant ATLAS analyses are given in Refs. [25, 27], whereas the corresponding CMS analyses are given in Refs. [28, 29]. However, as discussed in the introduction, in Ref. [40] a reinterpretation of the original ATLAS data in the context of a singlino/higgsino NMSSM scenario has been performed. We use their exclusion lines as given in Fig. 8 of Ref. [40] to exclude low mass points from our data sample. The relevant characteristics of our data sample and theirs, particularly the singlino content of the LSP of 90% or larger, see the next section, are identical. Here it should

be stressed again that the analysis presented in Ref. [40] did not include GUT-based values for the fermionic soft SUSY-breaking parameters, and hence our choices in this respect differ from theirs. However, this has no impact on the applicability of their limits on our data set, as $M_1 \sim M_2/2$ are much larger than μ and play only a minor role in the composition of the $\tilde{\chi}_{1,2,3}^0$ and $\tilde{\chi}_1^\pm$.

As a further check, we passed the points that fulfill all constraints, including the above described soft-lepton excesses through the code `SModelS-v3.1.0` [102]. We found that none of these points is excluded by `SModelS` [102–106], as expected from the fact that in the investigated parameter region the most relevant searches remain those focused on the 'compressed' EWino spectra, which lead exactly to the soft-lepton excesses. In this compressed mass region, searches for chargino pair production or associated chargino-neutralino production - resulting in two- or three high p_T leptons plus missing energy signals - are not as pertinent. On the other hand, since the slepton masses are fixed at 1 TeV in our analysis, see below, they are not constrained by direct slepton pair production, which would typically produce a two-lepton plus \cancel{E}_T signal.

4 Parameter scan and flow of the analysis

We employ the code `NMSSMTools` [53–56] as our spectrum generator³. It also computes the branching ratios (BRs) of the Higgs bosons, the Higgs effective couplings, and the BRs of the superpartners.

We scan the neutralino/chargino NMSSM parameter space, aiming at fully covering the regions of low mass neutralinos and charginos consistent with our chosen scenario. We also scan the Higgs and the scalar-top sector parameter space, where the Higgs sector is relevant for the DD constraints, and the stop sector higher-order corrections ensure that we find $m_{h_1} \sim 125$ GeV. The sleptons are assumed to be sufficiently heavy such that they do not play any relevant role in our analysis. We allow for two sign combinations of $(\mu \times M_1)$ and A_λ , while keeping M_1 positive to achieve the GUT conditions for $M_{1,2,3}$. In fact, we use M_2 as our input parameter for the gaugino sector, and let `NMSSMTools` impose the GUT conditions on the gaugino soft SUSY-breaking masses. Our singlino/higgsino scenario is defined as follows:

singlino/higgsino: singlino DM with higgsino dominated $\tilde{\chi}_{2,3}^0$, $\tilde{\chi}_1^\pm$:

$$\begin{aligned}
1000 \text{ GeV} &\leq 2 \times M_1 = M_2 = M_3/3 \leq 2000 \text{ GeV} , & 150 \text{ GeV} &< |\mu| < 300 \text{ GeV} , \\
1000 \text{ GeV} &= m_{\tilde{l}_L} = m_{\tilde{l}_R} , & A_e &= A_\mu = A_\tau = 0 , \\
5000 \text{ GeV} &= M_{\tilde{Q}_{1,2}} = M_{\tilde{u}_R, \tilde{d}_R, \tilde{c}_R, \tilde{s}_R} , & A_{u,d,c,s} &= 0 , \\
3000 \text{ GeV} &= M_{\tilde{Q}_3} = M_{\tilde{t}_R, \tilde{b}_R} , & A_b &= 0 , & 5000 \text{ GeV} &< A_t < 8000 \text{ GeV} , \\
-0.7 &\leq \kappa < 0.7 , & 0 &< \lambda < 5 , & 0.5 &\leq \tan \beta \leq 50 , \\
5 \text{ GeV} &\leq |A_\lambda| \leq 5000 \text{ GeV} , & -1000 \text{ GeV} &\leq A_\kappa \leq 1000 \text{ GeV} . & & (13)
\end{aligned}$$

³`NMSSMTools` contains code based on `HDECAY` [107, 108] and `SDECAY` [109].

Here $m_{\tilde{L},R}$ are the diagonal soft SUSY-breaking parameters in the slepton sector, identical for all three generations, with $A_{e,\mu,\tau}$ the corresponding trilinear couplings. $M_{\tilde{Q}_{1,2}}, M_{\tilde{u}_R, \tilde{d}_R, \tilde{c}_R, \tilde{s}_R}$ denote the diagonal soft SUSY-breaking parameters in the scalar quark sector of the first two generations, whereas $M_{\tilde{Q}_3}, M_{\tilde{t}_R, \tilde{b}_R}$ are for the third generations. The respective trilinear couplings are $A_{u,d,c,s}$ and $A_{t,b}$. All the $\overline{\text{DR}}$ parameters are defined at 3 TeV.

The data sample is generated by an in-house code that interfaces `NMSSMTools` with `MultiNest` [110], and that implements an ad-hoc likelihood, which includes most of the constraints described above, in order to drive the sampling algorithm into the phenomenologically acceptable regions. Spectra corresponding to parameter space points that are either compatible with the constraints, or not far from the allowed region, are saved into SLHA files [111, 112] for further processing.⁴

Moreover, in order to sample thoroughly and efficiently our scenario, we split the parameter range into hypercubes, as required by `MultiNest`, for each one of which we launch a separate instance of our sampling code. We also sampled multiple times each hypercube in order to increase the coverage of our sample.

As a second step, the SLHA files are further processed by running each point through `HiggsTools`, in order to check whether it satisfies or not the constraints coming from the characterization of h_1 (with $m_{h_1} \sim 125$ GeV), and the ones coming from searches for the Higgses of the extended scalar sector. The "allowed flag" from `HiggsBounds` and the χ^2 from `HiggsSignals` are saved into a custom `BLOCK` inside the SLHA file.

The processed SLHA files, which now also include the information on the compatibility with the Higgs sector constraints, are saved into `HDF5` archives for efficient storage and analysis.

As a last step, our analysis code processes these `HDF5` files, imposing the definitive set of constraints in a step-wise fashion to create the various point populations that we use to study the phenomenology of the scenario, and that are described in details in the next section. This applies in particular to the searches for the compressed spectra EWino searches, taken over from Ref. [40].

5 Results

We follow the analysis flow as described above and indicate the points surviving certain constraints with different colors:

- grey: all scan points that were saved at the sampling level; note that this includes points that are excluded by current constraints, although not all of them; however, it allows us to identify more clearly the region that was sampled by our code;
- blue: points that comply with the relic density constraints;

⁴We decide to save also points that are not allowed, albeit not all of them because of the limited resources available to us, in order to better understand how our code was exploring the parameter space.

- cyan: points that additionally pass the DD constraints, see Sect. 3;
- green: points that additionally satisfy the constraints implemented in `NMSSMTools`;
- purple: points that additionally pass `HiggsBounds`;
- pale orange: points that additionally pass `HiggsSignals`;
- bright orange: points for which additionally $10 \text{ GeV} < m_{\tilde{\chi}_2^0} - m_{\tilde{\chi}_1^0} < 35 \text{ GeV}$;
- red: points that additionally pass the LHC constraints from searches for $pp \rightarrow \tilde{\chi}_{2,3}^0 \tilde{\chi}_1^\pm$ with small Δm_{21} , while at the same time being candidate for the excesses that appear in the same searches.

We perform our analysis by projecting our multidimensional sample onto two-dimensional planes. Since the point density has no physical meaning by itself, but rather reflects the sampling dynamics, we bin the two-dimensional plane and color each cell according to the scheme above if there is at least one point contained in it.

We start our phenomenological analysis with the preferred parameter spaces found in our scan in the singlino/higgsino scenario. In the description of the plots we will focus on the red points, i.e. the ones that potentially describe the excesses observed at ATLAS and CMS. Only if the other levels of exclusion exhibit important information we will comment on them.

In Fig. 1 we show the coverage of our parameter scan in the singlino/higgsino scenario for the λ - κ plane. The plot demonstrates that λ and κ are forced into a narrow range of small values with a strong correlation among these two parameters. This is driven by the requirement to respect the DM relic density constraint, which selects values for which $\lambda \simeq 2\kappa$ (see, e.g., Ref. [40]). Concerning A_λ (not shown), it covers the whole scan range, whereas A_κ (not shown) is restricted to $|A_\kappa| \lesssim 350 \text{ GeV}$.

In Fig. 2 we show the main result of our parameter scan: the $m_{\tilde{\chi}_2^0} - \Delta m_{21}$ plane, overlaid with the experimental 95% CL exclusion bounds as recasted in Ref. [40]. The blue line indicates the ATLAS 3 soft-lepton limits [27], whereas the purple line indicates the ATLAS 2 soft-lepton limits [25].⁵ One can observe that our red points, i.e. the ones passing all constraints stretch out from the 95% CL exclusion lines up to $m_{\tilde{\chi}_2^0} = 250 \text{ GeV}$, where our scan stopped. $\Delta m_{21} := m_{\tilde{\chi}_2^0} - m_{\tilde{\chi}_1^0}$ is found between 10 GeV (where we cut the “preferred parameter space”) and $\sim 16 \text{ GeV}$, with the values closest to the exclusion bounds of $12 \text{ GeV} \lesssim \Delta m_{21} \lesssim 14 \text{ GeV}$. This plot clearly demonstrates that the singlino/higgsino scenario in the NMSSM yields a very good description of the soft-lepton excesses observed at ATLAS and CMS, while being in agreement with all other theoretical and experimental constraints.

The fact that Δm_{21} comes out somewhat smaller in the NMSSM as compared to the preferred $\sim 20 \text{ GeV}$ in the MSSM (see, e.g., Ref. [30]) can be attributed to the fact that two production

⁵The recasting performed in Ref. [40] was performed only for the ATLAS limits. However, it has been discussed in the literature, see e.g. Ref. [30], that the ATLAS and CMS limits effectively show the same excesses in the 3 and 2 soft-lepton channels.

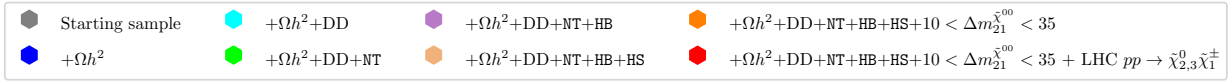
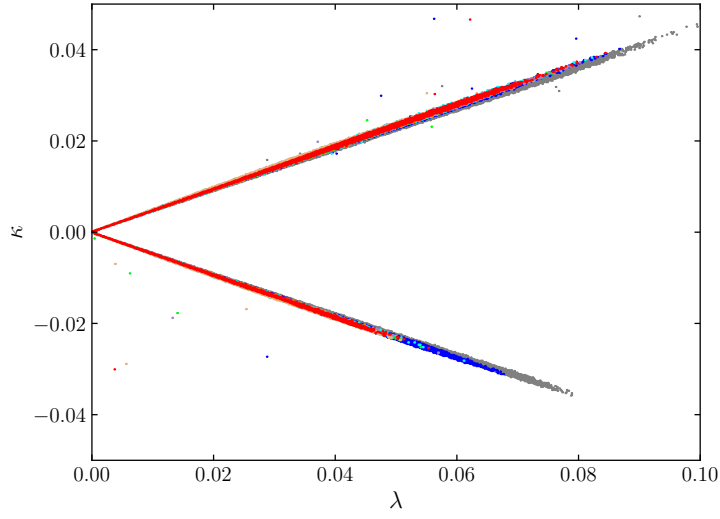


Figure 1: The results of our parameter scan in the singlino/higgsino scenario in the λ - κ plane.

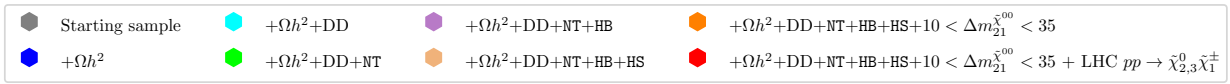
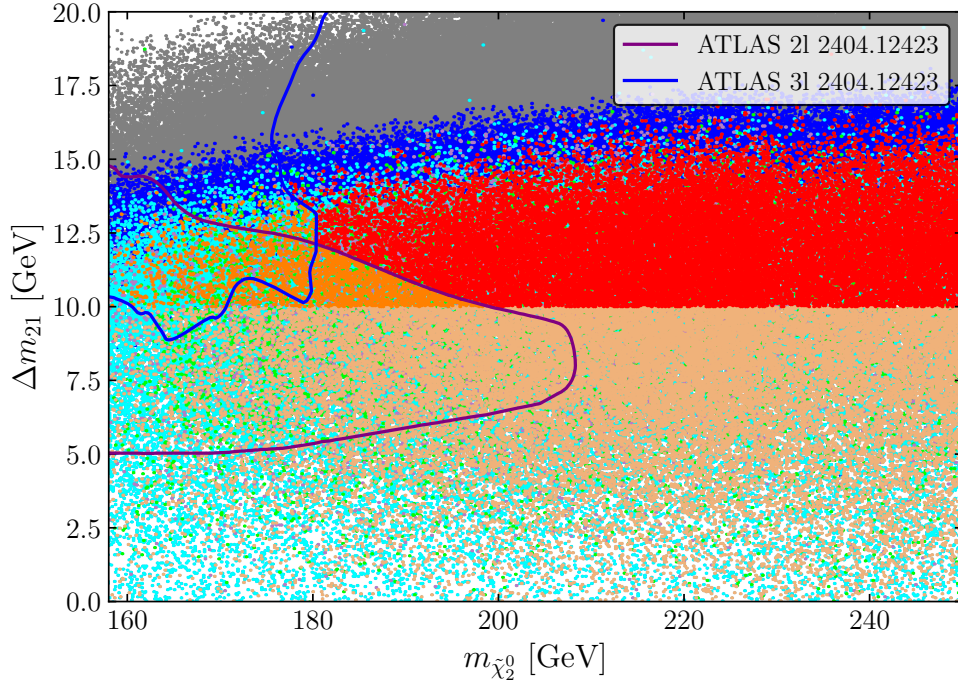


Figure 2: The results of our parameter scan in the singlino/higgsino scenario in the $m_{\tilde{\chi}_2^0}$ - Δm_{21} plane.

channels are open in the NMSSM, $pp \rightarrow \tilde{\chi}_{2,3}^0 \tilde{\chi}_1^\pm$, as compared to only one in the MSSM, where by definition we have $m_{\tilde{\chi}_3^0} > m_{\tilde{\chi}_2^0}$. This is quantified in the left plot of Fig. 3, where we show the results of our scan in the $m_{\tilde{\chi}_2^0} - (m_{\tilde{\chi}_3^0} - m_{\tilde{\chi}_2^0})$ plane. One can see that the preferred parameter space has $3 \text{ GeV} \lesssim m_{\tilde{\chi}_3^0} - m_{\tilde{\chi}_2^0} \lesssim 13 \text{ GeV}$, leading to a correspondingly larger difference in $m_{\tilde{\chi}_3^0} - m_{\tilde{\chi}_1^0}$. In the right plot of Fig. 3 we show our scan results in the $m_{\tilde{\chi}_2^0} - (m_{\tilde{\chi}_2^0} - m_{\tilde{\chi}_1^\pm})$ plane. Here one can observe that the lightest chargino is up to $\sim 5 \text{ GeV}$ heavier than the second lightest neutralino.

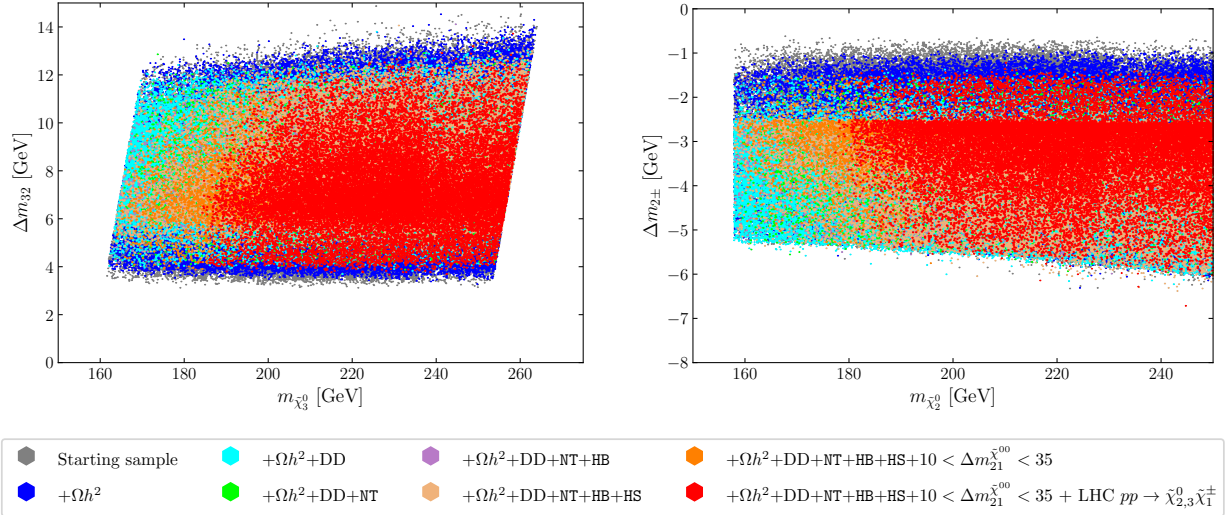


Figure 3: The results of our parameter scan in the singlino/higgsino scenario in the $m_{\tilde{\chi}_2^0} - (m_{\tilde{\chi}_3^0} - m_{\tilde{\chi}_2^0})$ plane (left) and the $m_{\tilde{\chi}_2^0} - (m_{\tilde{\chi}_2^0} - m_{\tilde{\chi}_1^\pm})$ plane (right).

In Fig. 4 we show our predictions for $\sigma(pp \rightarrow \tilde{\chi}_2^0 \tilde{\chi}_1^\pm) + \sigma(pp \rightarrow \tilde{\chi}_3^0 \tilde{\chi}_1^\pm)$ at the LHC at $\sqrt{s} = 13 \text{ TeV}$ in the $m_{\tilde{\chi}_2^0} - \Delta m_{21}$ plane. The combined cross-section underscores that contributions from both Higgsino-like NLSPs, $\tilde{\chi}_2^0$ and $\tilde{\chi}_3^0$ are relevant for the signal channel. We computed the leading-order (LO) production cross-section using `MadGraph (MG5aMC)-v3.6.3` [113] for which we incorporated the NMSSM model file from the `FeynRules` [114, 115] database. The SLHA files, generated from our `NMSSMTools` run and validated against all relevant constraints, were passed as `MadGraph` param-cards. To obtain the NLO cross-section, we applied the MSSM k-factor given by `Resummino` [116–120] to the LO production cross-section. We assume the QCD loop effects in both the NMSSM and MSSM production cross-sections to be of similar order. The size of the cross section for each point is indicated by the color scale. One can see that the cross section mainly depends on $m_{\tilde{\chi}_2^0} \approx m_{\tilde{\chi}_1^\pm}$, but is nearly independent on Δm_{21} : while an increasing mass of the final state particles leads to smaller cross sections, Δm_{21} has only a small impact on the mixings of $\tilde{\chi}_2^0$ and thus its couplings entering the cross section calculation. The smallest EWino masses yield production cross sections of approximately $\sim 1.3 \text{ pb}$, going down to $\sim 0.7 \text{ pb}$ for $m_{\tilde{\chi}_2^0} \sim 200 \text{ GeV}$ (where our plot ends). These values are roughly consistent with the cross sections required to reproduce the observed excess in events, within the associated uncertainties, see e.g. the discussion in Ref. [30]. On the other hand, this defines a clear target for Run 3 of the LHC and future collider stages. Although no dedicated projections for the discovery potential at the HL-LHC

are currently available, it appears plausible that Run 3 could provide valuable insights into the proposed explanation of the soft-lepton excesses.

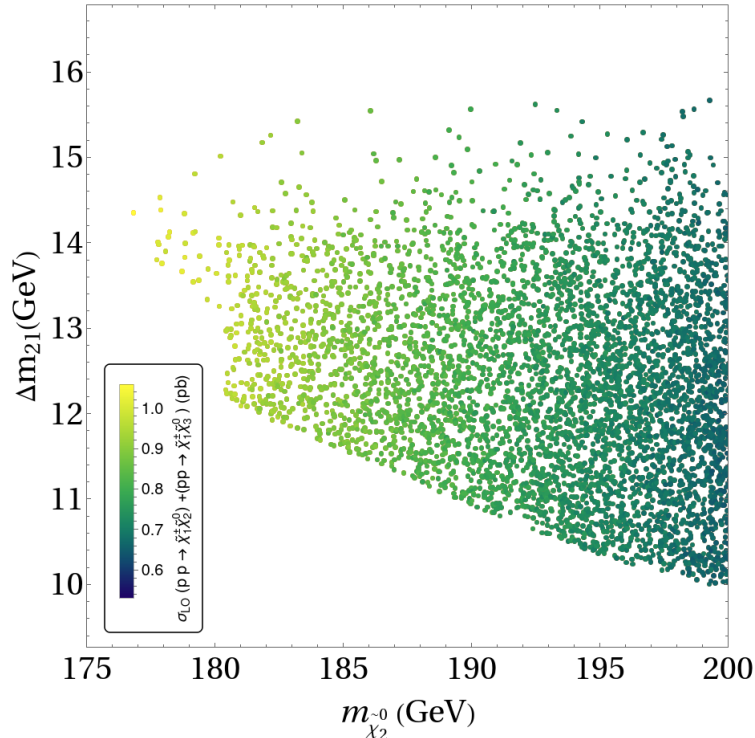


Figure 4: The predictions of $\sigma(pp \rightarrow \tilde{\chi}_2^0 \tilde{\chi}_1^\pm) + \sigma(pp \rightarrow \tilde{\chi}_3^0 \tilde{\chi}_1^\pm)$ (see text) are shown as color coding in the $m_{\tilde{\chi}_2^0} - \Delta m_{21}$ plane.

In Fig. 5, we present our results in the $\lambda - \Delta m_{21}$ plane (left) and the $\kappa - \Delta m_{21}$ plane (right). It can be seen that larger values of Δm_{21} are attained for higher λ , although the dependence remains relatively mild. The preferred region corresponds to $0.03 \lesssim \lambda \lesssim 0.08$. In contrast, no clear trend is observed for κ , apart from a dip in the (red) allowed parameter space that excludes κ values near zero for the largest Δm_{21} .

We now turn to the results for other particle masses in our scan. As discussed above, the scalar leptons and quarks are chosen to be heavy, and we do not present any results for them here. On the other hand, the heavy NMSSM Higgs-boson masses are effectively treated as free parameters, subject to the BSM Higgs searches as implemented into `HiggsBounds` as well as the LHC Higgs-boson rate measurements as implemented into `HiggsSignals`. In Fig. 6 we show the results of our scan in the $m_{A_2} - \tan \beta$ plane (left) and the $m_{H^\pm} - \tan \beta$ plane (right). In the left plot one can see that m_{A_2} ranges from ~ 1000 GeV up to values $\gtrsim 7.5$ TeV for $\tan \beta = 50$, where our scan stopped. However, one can clearly observe the parameter space that is excluded by the BSM Higgs-boson searches, starting at $m_{A_2} \sim 1000$ GeV and $\tan \beta \sim 10$. A small region of purple points is visible at low $\tan \beta$ for $m_{A_2} \lesssim 1000$ GeV, where points are excluded by `HiggsSignals`. The large cyan region visible for lower m_{A_2} values and $\tan \beta \gtrsim 10$ are excluded by the searches for $pp \rightarrow \phi \rightarrow \tau\tau$, with ϕ being a heavy \mathcal{CP} -even or \mathcal{CP} -odd Higgs boson. Apart from this, no specific restriction on the heavy \mathcal{CP} -odd Higgs-boson mass can be identified, implying that no clear prediction for future collider

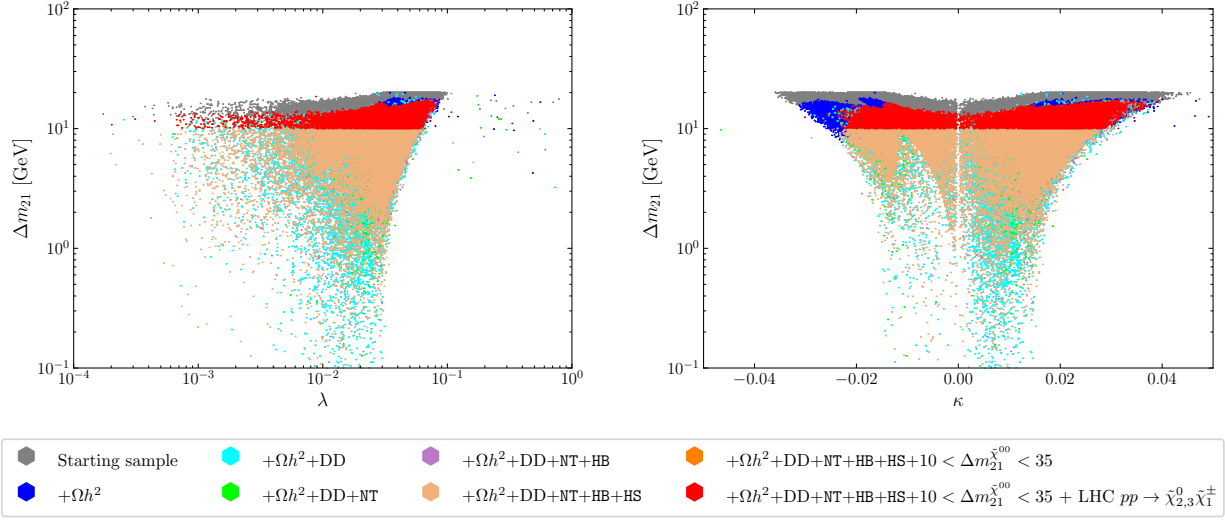


Figure 5: The results of our parameter scan in the singlino/higgsino scenario in the λ - Δm_{21} plane (left) and the κ - Δm_{21} plane (right).

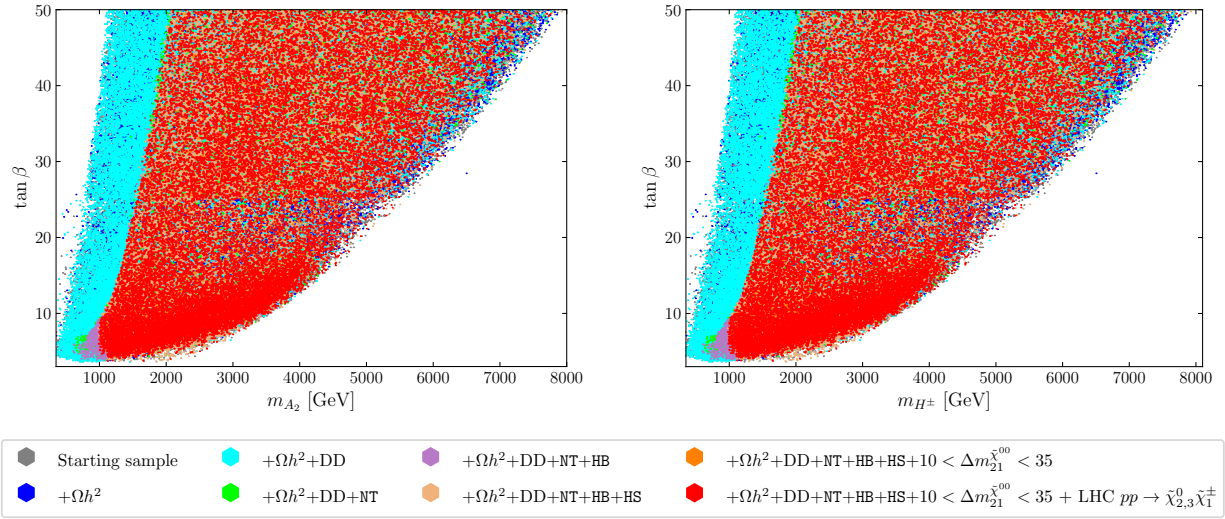


Figure 6: The results of our parameter scan in the singlino/higgsino scenario in the m_{A_2} - $\tan \beta$ plane (left) and the m_{H^\pm} - $\tan \beta$ plane (right).

searches can be made. The charged Higgs-boson mass, shown in the right panel of the figure, is strongly correlated with the neutral Higgs-boson masses and therefore exhibits a similar behavior. However, the direct limits on charged Higgs bosons are less stringent than those on neutral Higgs bosons, and the observed constraints on the charged Higgs sector mainly originate from searches targeting the neutral Higgs bosons.

In Fig. 7 we turn to the lighter \mathcal{CP} -even masses in our scan. In the left plot we show the results in the m_{h_1} - $|S_{13}|^2$ plane, i.e. the light \mathcal{CP} -even Higgs-boson mass together with its singlet component. We find $122 \text{ GeV} \lesssim m_{h_1} \lesssim 128 \text{ GeV}$, as required by the LHC Higgs-boson

measurements (and here enforced by, taking into account a 3 GeV theory uncertainty [121]). The singlet component is always smaller than 10% (with even smaller values for m_{h_1} close to the allowed lower and upper limits). Also these small values are imposed by `HiggsSignals` and ensure the agreement with the LHC measurements. The right plot shows the m_{h_2} - $|S_{23}|^2$ plane, i.e. the second lightest \mathcal{CP} -even Higgs-boson mass together with its singlet component. We find that the mass is restricted to be $125 \text{ GeV} \lesssim m_{h_2} \lesssim 225 \text{ GeV}$, with a singlet component of 90% or larger. This indicates that the soft-lepton excesses at ATLAS and CMS, when interpreted in the NMSSM, predict a second light Higgs-boson, which, however, largely decouples from the SM particles. Nevertheless, this light Higgs-boson might be an interesting target for future HL-LHC direct searches. We leave a detailed phenomenological analysis for future work.

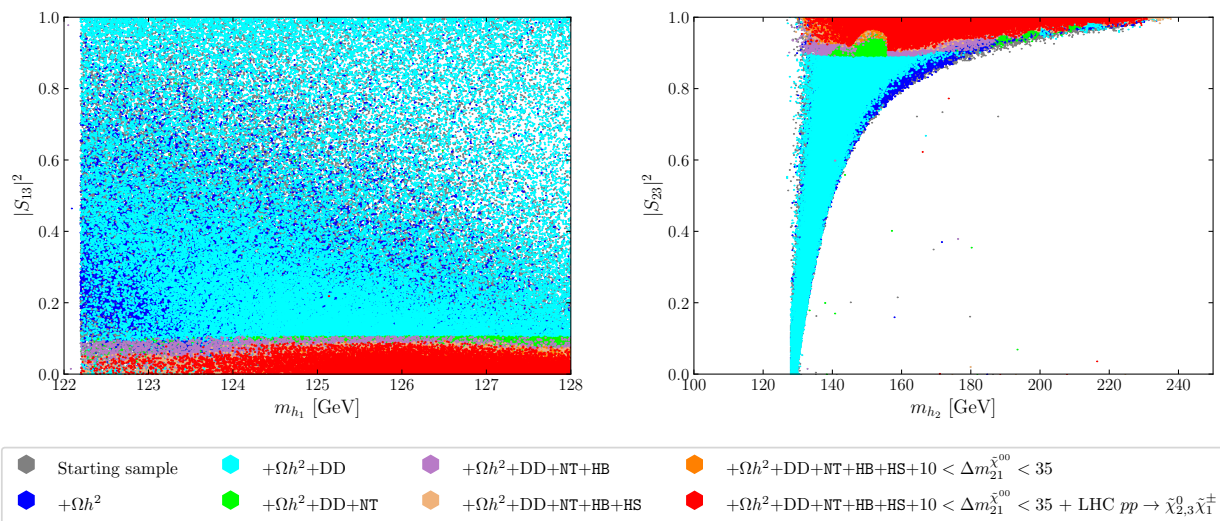


Figure 7: The results of our parameter scan in the singlino/higgsino scenario in the m_{h_1} - $|S_{13}|^2$ plane (left) and the m_{h_2} - $|S_{23}|^2$ plane (right).

We finish our analysis of the \mathcal{CP} -even Higgs bosons with Fig. 8, where we show $g_{\gamma\gamma}$ as a function of $m_{\tilde{\chi}_1^\pm}$. $g_{\gamma\gamma}$ is the effective coupling of the h_1 to two photons, and it is affected by the contributions from light charged particles that would appear in loop diagrams in the full theory. The lightest chargino naturally can contribute to a deviation of $g_{\gamma\gamma}$ from unity. However, one can observe that this deviation hardly exceeds the 5% level, and the predicted rate of $h_1 \rightarrow \gamma\gamma$ is close to the SM prediction, and thus in agreement with the experimental data. However, part of this parameter space which features relatively small deviations will be probed by HL-LHC and future colliders. On the other hand, it is apparent that parameter points indistinguishable from the SM at any foreseen experiment are also possible.

Now we turn to the predictions for DM in our singlino/higgsino scenario. In Fig. 9 we present our scan results in the Δm_{21} - $\Omega_\chi h^2$ plane. A clear correlation over the whole scanned parameter space is visible, with lower DM relic densities reached for smaller Δm_{21} . Turning this around, larger Δm_{21} , as favored by the soft-lepton excesses leads naturally to a (possible) saturation of the DM relic density. This is in stark contrast to the higgsino scenarios in the MSSM, see Ref. [30], where always a strongly underabundant DM relic density was found.

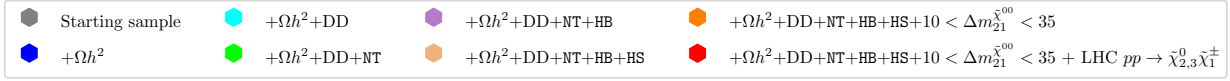
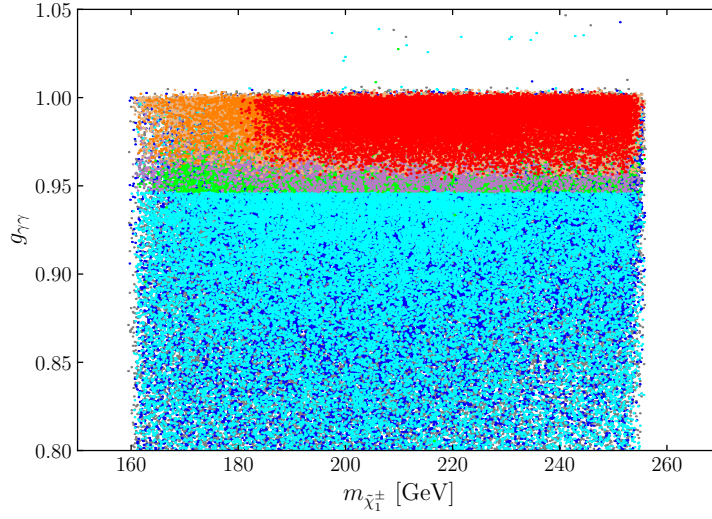


Figure 8: The results of our parameter scan in the singlino/higgsino scenario in the $m_{\tilde{\chi}_1^\pm}$ - $g_{\gamma\gamma}$ plane.

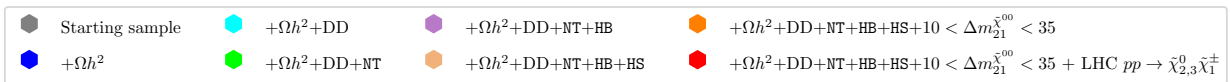
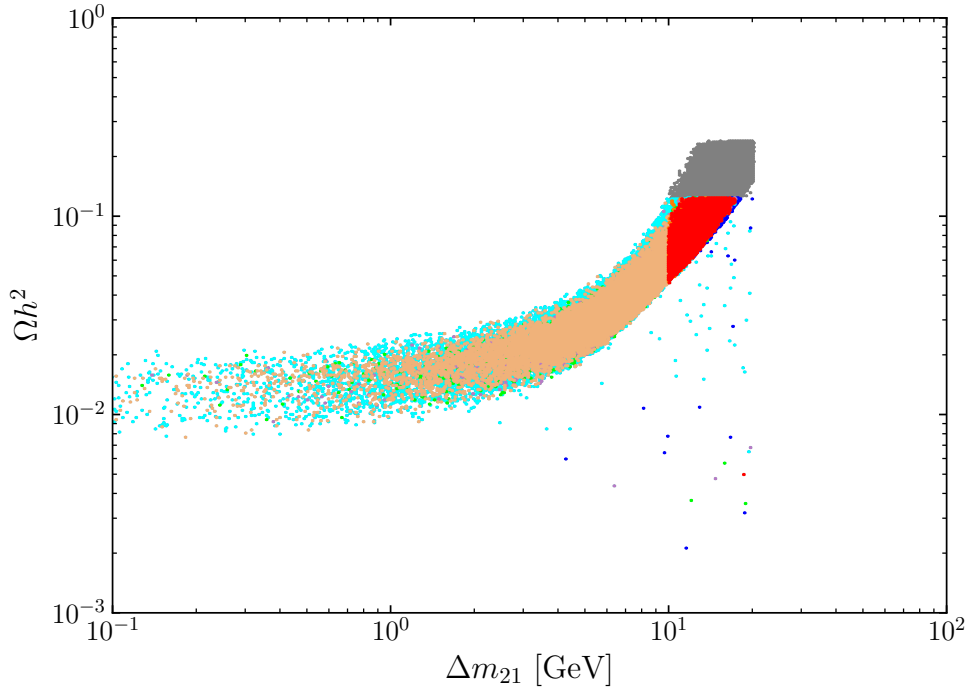


Figure 9: The results of our parameter scan in the singlino/higgsino scenario in the Δm_{21} - $\Omega_\chi h^2$ plane.

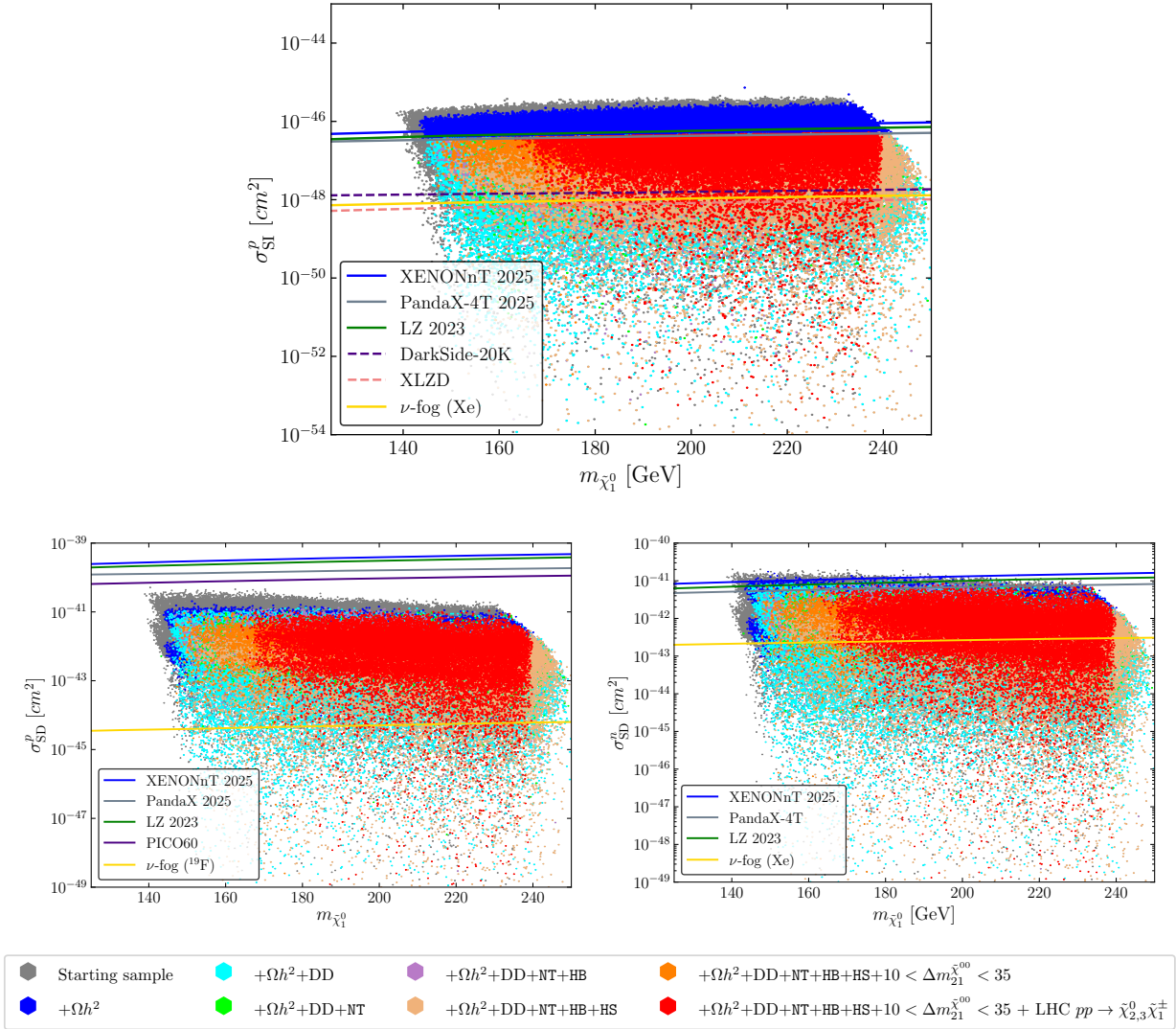


Figure 10: The results of our parameter scan in the singlino/higgsino scenario in the $m_{\tilde{\chi}_1^0}$ - σ_{SI}^p plane (upper plot) and the $m_{\tilde{\chi}_1^0}$ - σ_{SD}^p plane (lower left plot) and the $m_{\tilde{\chi}_1^0}$ - σ_{SD}^n plane (lower right plot)

The prospects for spin-independent (σ_{SI}^p) and spin-dependent (σ_{SD}^p , σ_{SD}^n for p and n scattering, respectively) direct DM searches in our singlino/higgsino scenario are presented in Fig. 10. All plots show the respective cross section as a function of the DM mass, $m_{\tilde{\chi}_1^0}$. In the upper plot we show σ_{SI}^p and indicate with solid blue, black and gray lines the current bounds from XENON-nT [83], PandaX-4T [81] and LZ [82], respectively. As discussed in Sect. 3 and visible in the plot, we applied the limits from PandaX-4T [81]. Having applied the more recent published limits from LZ [82] would cut away the points with the highest DD cross sections. However, we do not expect a major relevant impact on our general findings. As dashed purple and red lines we indicate the anticipated limits from DarkSide-20K [122] and XLZD [123], respectively. The ν -fog (for Xenon) [124, 125] is shown as yellow solid line. While the future experiments can cover a large part of the preferred parameter space,

the NMSSM interpretation of the 2- and 3-soft lepton excesses are also compatible with points predicting a DD cross section below the ν -fog limit, i.e. not observable with currently used experimental set-ups (see also Ref. [126] for a recent analysis of higgsino DM in DD experiments). We have tested that the points below the ν -fog limit correspond to somewhat smaller Δm_{21} , not exceeding 13 GeV for the smallest allowed $m_{\tilde{\chi}_2^0}$ values. In the lower row of Fig. 10 on the left (right) we present the results for the spin-dependent scattering cross section with protons (neutrons). The blue, gray and green solid lines indicate the limits from XENON-nT [83], PandaX-4T [81] and LZ [82], respectively. In the left plot we indicate additionally the limit from PICO60 [127] as solid black line. The yellow solid lines show the ν -fog limits for ^{19}F (left) and Xenon (right) [124, 125]. One can observe that the SD cross section with protons is predicted to be far below any current bounds, and can also reach below the ^{19}F ν -fog limit. On the other hand, the SD scattering with neutrons reaches the strongest experimental limit, as currently given by PandaX-4T, which cuts away a couple of points of our scan. Also this cross section reaches well below the Xenon ν -fog limit. Overall, while the DD experiments show interesting prospects for the future runs, the NMSSM singlino/higgsino explanation of the soft lepton excesses may well escape this kind of experimental test (in contrast to the MSSM explanations presented in Ref. [30]).

6 Conclusions

The EW sector of the NMSSM, consisting of five neutralinos, $\tilde{\chi}_{1,2,3,4,5}^0$ and two charginos, $\tilde{\chi}_{1,2}^\pm$ (as well as the SUSY partners of the SM leptons), can account for a variety of experimental data that cannot be described by the SM. In particular, assuming that the lightest neutralino, $\tilde{\chi}_1^0$, is the LSP, this particle constitutes a DM candidate in good agreement with the observed limits on the DM relic density of the universe, as well as with negative results from direct detection experiments.

At the LHC, a wide range of experimental searches are carried out to search for the production and decays of the EWinos in various final states, often performed in the context of the MSSM. In particular, the “golden channel”, $pp \rightarrow \tilde{\chi}_2^0, \tilde{\chi}_1^\pm \rightarrow \tilde{\chi}_1^0 Z^{(*)} \tilde{\chi}_1^0 W^{\pm(*)}$ is used to place stringent constraints on the EW MSSM parameter space (where sleptons are assumed to be heavy). The targeted final states contain two or three (possibly soft) leptons accompanied by a substantial amount of \cancel{E}_T . These searches are particularly challenging in the part of the parameter space where the mass differences between the final and the initial state EWinos become small, leading to rather soft final state leptons. Despite these experimental challenges, the CMS and ATLAS collaborations are searching actively for EWinos in this “compressed spectra” region, focusing on the 2 and 3 soft-lepton plus \cancel{E}_T final state. Interestingly, the experimental data of searches in the “golden channel”, $pp \rightarrow \tilde{\chi}_2^0 \tilde{\chi}_1^\pm \rightarrow \tilde{\chi}_1^0 Z^* \tilde{\chi}_1^0 W^{\pm*}$ show consistent excesses between CMS and ATLAS in exactly these final states [25, 27–29]. These searches assume a simplified model scenario with $m_{\tilde{\chi}_2^0} \approx m_{\tilde{\chi}_1^\pm}$ and $\Delta m_{21} := m_{\tilde{\chi}_2^0} - m_{\tilde{\chi}_1^0} \approx \mathcal{O}(20 \text{ GeV})$. The sleptons are assumed to be relatively heavy, and thus to not take part in the decays of the initially produced EWinos.

In Ref. [30] within the MSSM three different scenarios were analyzed, classified by the

hierarchy and signs of the EWino mass parameters, M_1 , M_2 and μ , while assuming heavy sleptons. It was found that the MSSM scenarios that give a good description of the soft-lepton excesses and complying with the DM experimental constraints, require $|M_1| \sim |M_2|$. However, one of the most compelling arguments in favor of SUSY is the unification of forces at the GUT scale, yielding (in simple GUT realization) the following mass pattern at the EW scale: $M_1 \sim M_2/2 \sim M_3/6$, where M_3 is the gluino mass, $m_{\tilde{g}}$. Searches for colored particles at the LHC have set a limit of $m_{\tilde{g}} \gtrsim 2$ TeV (if not for very small $m_{\tilde{g}} - m_{\tilde{\chi}_1^0}$), placing a lower bound of $|M_1| \gtrsim 350$ GeV. Consequently, the MSSM scenarios that can describe the soft-lepton excesses do not follow the GUT-based mass pattern.

In this paper we propose a scenario that can describe well the soft-lepton excesses, follows the GUT-based mass patterns and is in agreement with the searches for gluinos, the singlino/higgsino scenario: the NMSSM with a singlino dominated LSP, with $200 \text{ GeV} \approx |\mu| < M_1 \sim M_2/2 \sim M_3/6$, and $m_{\tilde{g}} \gtrsim 2$ TeV. This parameter space corresponds to higgsino-like $\tilde{\chi}_{2,3}^0$ and $\tilde{\chi}_1^\pm$. The LHC searches are interpreted as searches for $pp \rightarrow \tilde{\chi}_{2,3}^0 \tilde{\chi}_1^\pm \rightarrow \tilde{\chi}_1^0 Z^* \tilde{\chi}_1^0 W^{\pm*}$ in the NMSSM, leading to the desired 2 or 3 soft-lepton plus \cancel{E}_T final states.

We scanned over the relevant NMSSM parameter space, employing the GUT relation $M_1 \sim M_2/2 \sim M_3/6$, with $|\mu| \leq M_1$ and $M_1 \geq 350$ GeV. We have taken into account all relevant experimental constraints: the DM relic density, the DD cross section limits (the indirect detection limits do not play a role), flavor observables, the LHC BSM Higgs-boson searches, and the LHC Higgs-boson rate measurements (where we identify the lightest \mathcal{CP} -even Higgs boson with the Higgs discovered at the LHC). In particular, we apply the limits from the 2 and 3 soft-lepton searches (making use of the NMSSM reinterpretation given in Ref. [40]). We demonstrated that the singlino/higgsino scenario can yield a perfect description of the observed soft-lepton excesses, while being in agreement with all existing constraint and fulfilling the GUT relations for $M_{1,2,3}$.

The preferred mass ranges are $m_{\tilde{\chi}_2^0} \gtrsim 180$ GeV, $\Delta m_{21} := m_{\tilde{\chi}_2^0} - m_{\tilde{\chi}_1^0} \approx 12 - 14$ GeV, $m_{\tilde{\chi}_3^0} - m_{\tilde{\chi}_2^0} \approx 3 - 13$ GeV, $m_{\tilde{\chi}_1^\pm} - m_{\tilde{\chi}_2^0} \approx 0 - 5$ GeV. In the lower mass range the golden channel has a production cross section in the order of one pb. The singlino/higgsino scenario furthermore predicts a second lightest \mathcal{CP} -even Higgs boson in the range of $125 \lesssim m_{h_2} \lesssim 225$ GeV with a singlet component larger than 0.9, which may yield interesting prospects for the HL-LHC. The singlino/higgsino scenario can yield the full DM content of the universe. The future DD searches show interesting prospects for the next experimental runs, in particular for the spin independent searches. However, for all types of DD searches (spin independent, spin dependent with protons or neutrons) we find parameter points that are below the respective ν -fog limits and may thus escape the searches (using the established experimental techniques).

We have also studied whether it would be possible to probe these scenarios via the characterization of the h_1 , i.e. the lightest \mathcal{CP} -even Higgs boson of the NMSSM, which is interpreted as the Higgs-boson discovered at the LHC. A prime target for this approach is the decay of the $h_1 \rightarrow \gamma\gamma$. We have found that, while non-negligible deviations from the SM are possible for the effective coupling to two photons, there are regions of the preferred parameter space that features experimentally indistinguishable deviation with respect to the SM. In other

words, while the observation of a small deviation in $h_1 \rightarrow \gamma\gamma$ can very well be explained in our scenario, it will not be possible to use these measurements to completely test it. On the other hand, the search for the other Higgs states of the NMSSM appear as an interesting target. We leave such an analysis for a future study.

For the first time, CMS and ATLAS observe consistent excesses in the search for SUSY particles. These excesses are observed in the processes $pp \rightarrow \tilde{\chi}_2^0 \tilde{\chi}_1^\pm \rightarrow \tilde{\chi}_1^0 Z^* \tilde{\chi}_1^0 W^*$: 2 soft leptons plus \cancel{E}_T , and 3 soft leptons plus \cancel{E}_T . While each experiment and search individually is not significant by itself, the occurrence of excesses in multiple search channels, observed by both CMS and ATLAS, gives rise to the hope that indeed for the first time BSM physics has been observed. The LHC Run 3 should give conclusive results, either refuting the observed excesses, or discovering SUSY.

Acknowledgments

We thank M. Martinez for helpful discussions. I.S. acknowledges support from SERB-MATRICES, ANRF, India, under grant no. MTR/2023/000715. The work of S.H. has received financial support from the grant PID2019-110058GB-C21 funded by MCIN/AEI/10.13039/501100011033 and by ‘‘ERDF A way of making Europe’’, and in part by the grant IFT Centro de Excelencia Severo Ochoa CEX2020-001007-S funded by MCIN/AEI/10.13039/501100011033. S.H. also acknowledges support from Grant PID2022-142545NB-C21 funded by MCIN/AEI/10.13039/501100011033/ FEDER, UE. E.B. would like to thank the LNF INFN Data Cloud Team and the CERN-IT department for the use of their computational resources.

References

- [1] H. Nilles, *Phys. Rept.* **110** (1984) 1.
- [2] R. Barbieri, *Riv. Nuovo Cim.* **11** (1988) 1.
- [3] H. Haber, G. Kane, *Phys. Rept.* **117** (1985) 75.
- [4] J. Gunion, H. Haber, *Nucl. Phys.* **B 272** (1986) 1.
- [5] S. Heinemeyer and C. Muñoz, *Universe* **8** (2022) no.8, 427.
- [6] H. Goldberg, *Phys. Rev. Lett.* **50** (1983) 1419.
- [7] J. Ellis, J. Hagelin, D. Nanopoulos, K. Olive, M. Srednicki, *Nucl. Phys.* **B 238** (1984) 453.
- [8] J.E. Kim and H.P. Nilles, *Phys. Lett.* **B 138** (1984) 150.
- [9] M. Maniatis, *Int. J. Mod. Phys.* **A 25** (2010) 3505 [arXiv:0906.0777 [hep-ph]].

- [10] Ulrich Ellwanger, Cyril Hugonie, and A.M.Teixeira, *Phys.Rept.* **496** (2010) 1 [arXiv:0910.1785 [hep-ph]].
- [11] See: <https://twiki.cern.ch/twiki/bin/view/AtlasPublic/SupersymmetryPublicResults> .
- [12] See: <https://twiki.cern.ch/twiki/bin/view/CMSPublic/PhysicsResultsSUS> .
- [13] D. A. Dicus, S. Nandi and X. Tata, *Phys. Lett.* **B 129** (1983), 451 [erratum: *Phys. Lett.* **B 145** (1984), 448].
- [14] A. H. Chamseddine, P. Nath and R. L. Arnowitt, *Phys. Lett.* **B 129** (1983), 445 [erratum: *Phys. Lett.* **B 132** (1983), 467].
- [15] H. Baer and X. Tata, *Phys. Lett.* **B 155** (1985), 278-283.
- [16] H. Baer, K. Hagiwara and X. Tata, *Phys. Rev.* **D 35** (1987), 1598.
- [17] H. Baer, K. Hagiwara and X. Tata, *Phys. Rev. Lett.* **57** (1986), 294.
- [18] T. Buanes, I. Lara, K. Rolbiecki and K. Sakurai, *Phys. Rev. D* **107** (2023) no.9, 095021 [arXiv:2208.04342 [hep-ph]].
- [19] L. M. Carpenter, H. Gilmer, J. Kawamura and T. Murphy, *Phys. Rev. D* **109** (2024) no.1, 015012 [arXiv:2309.07213 [hep-ph]].
- [20] H. Baer, C. h. Chen, F. Paige and X. Tata, *Phys. Rev.* **D 50** (1994), 4508-4516 [arXiv:hep-ph/9404212 [hep-ph]].
- [21] H. Baer, V. Barger and P. Huang, *JHEP* **11** (2011), 031 [arXiv:1107.5581 [hep-ph]].
- [22] M. Abdughani and L. Wu, *Eur. Phys. J. C* **80** (2020) no.3, 233 [arXiv:1908.11350 [hep-ph]].
- [23] E. Bagnaschi *et al.*, *Eur. Phys. J. C* **78** (2018) no.3, 256 [arXiv:1710.11091 [hep-ph]].
- [24] P. Athron *et al.* [GAMBIT], *Eur. Phys. J. C* **79** (2019) no.5, 395 [arXiv:1809.02097 [hep-ph]].
- [25] G. Aad *et al.* [ATLAS], *Phys. Rev.* **D 101** (2020) no.5, 052005 [arXiv:1911.12606 [hep-ex]].
- [26] A. Tumasyan *et al.* [CMS], *JHEP* **04** (2022), 091 [arXiv:2111.06296 [hep-ex]].
- [27] G. Aad *et al.* [ATLAS], *Eur. Phys. J. C* **81** (2021) no.12, 1118 [arXiv:2106.01676 [hep-ex]].
- [28] A. Hayrapetyan *et al.* [CMS], arXiv:2402.01888 [hep-ex];
- [29] V. Chekhovsky *et al.* [CMS], [arXiv:2508.13900 [hep-ex]].

- [30] M. Chakraborti, S. Heinemeyer and I. Saha, *Eur. Phys. J. C* **84** (2024) no.8, 812 [arXiv:2403.14759 [hep-ph]].
- [31] N. Aghanim *et al.* [Planck Collaboration], *Astron. Astrophys.* **641** (2020), A6 [erratum: *Astron. Astrophys.* **652** (2021), C4] [arXiv:1807.06209 [astro-ph.CO]].
- [32] J. Aalbers *et al.* [LZ], *Phys. Rev. Lett.* **131** (2023) no.4, 041002 [arXiv:2207.03764 [hep-ex]].
- [33] M. Chakraborti, S. Heinemeyer and I. Saha, *Eur. Phys. J. C* **80** (2020) 10, 984 [arXiv:2006.15157 [hep-ph]].
- [34] M. Chakraborti, S. Heinemeyer and I. Saha, *Eur. Phys. J. C* **81** (2021) no.12, 1069 [arXiv:2103.13403 [hep-ph]].
- [35] M. Chakraborti, S. Heinemeyer and I. Saha, *Eur. Phys. J. C* **81** (2021) no.12, 1114 [arXiv:2104.03287 [hep-ph]].
- [36] M. Chakraborti, S. Heinemeyer, I. Saha and C. Schappacher, *Eur. Phys. J. C* **82** (2022) no.5, 483 [arXiv:2112.01389 [hep-ph]].
- [37] E. Bagnaschi, M. Chakraborti, S. Heinemeyer, I. Saha and G. Weiglein, *Eur. Phys. J. C* **82** (2022) no.5, 474 [arXiv:2203.15710 [hep-ph]].
- [38] M. Chakraborti, S. Heinemeyer and I. Saha, *Eur. Phys. J. C* **84** (2024) no.2, 165 [arXiv:2308.05723 [hep-ph]].
- [39] U. Ellwanger, C. Hugonie, S. F. King and S. Moretti, *Eur. Phys. J. C* **84**, no.8, 788 (2024) [arXiv:2404.19338 [hep-ph]].
- [40] D. Agin, B. Fuks, M. D. Goodsell and T. Murphy, *Eur. Phys. J. C* **84**, no.11, 1218 (2024) [arXiv:2404.12423 [hep-ph]].
- [41] S. P. Martin, *Phys. Rev. D* **109**, no.9, 095045 (2024) [arXiv:2403.19598 [hep-ph]].
- [42] D. Agin, B. Fuks, M. D. Goodsell and T. Murphy, *Eur. Phys. J. C* **85**, no.10, 1145 (2025) [arXiv:2506.21676 [hep-ph]].
- [43] A. Hammad, R. Ramos, A. Chakraborty, P. Ko and S. Moretti, [arXiv:2508.13912 [hep-ph]].
- [44] J. Y. Araz, B. Fuks, M. D. Goodsell and T. Murphy, [arXiv:2507.08927 [hep-ph]].
- [45] L. Constantin, S. Kraml, A. Lessa, T. Reymermier and W. Waltenberger, [arXiv:2512.14502 [hep-ph]].
- [46] M. D. Goodsell, [arXiv:2406.10042 [hep-ph]].
- [47] U. Amaldi, W. de Boer and H. Furstenau, *Phys. Lett. B* **260** (1991), 447-455.

- [48] G. L. Kane, C. F. Kolda, L. Roszkowski and J. D. Wells, *Phys. Rev. D* **49** (1994) 6173 [arXiv:hep-ph/9312272]; H. Baer and M. Brhlik, *Phys. Rev. D* **53** (1996) 597 [arXiv:hep-ph/9508321]; *Phys. Rev. D* **57** (1998) 567 [arXiv:hep-ph/9706509]; J. R. Ellis, T. Falk, K. A. Olive and M. Schmitt, *Phys. Lett. B* **388** (1996) 97 [arXiv:hep-ph/9607292]; *Phys. Lett. B* 413 (1997) 355 [arXiv:hep-ph/9705444]; J. R. Ellis, T. Falk, G. Ganis, K. A. Olive and M. Schmitt, *Phys. Rev. D* **58** (1998) 095002 [arXiv:hep-ph/9801445]; V. D. Barger and C. Kao, *Phys. Rev. D* **57** (1998) 3131 [arXiv:hep-ph/9704403]; J. R. Ellis, T. Falk, G. Ganis and K. A. Olive, *Phys. Rev. D* **62** (2000) 075010 [arXiv:hep-ph/0004169]; J. R. Ellis, T. Falk, G. Ganis, K. A. Olive and M. Srednicki, *Phys. Lett. B* **510** (2001) 236 [arXiv:hep-ph/0102098]; V. D. Barger and C. Kao, *Phys. Lett. B* **518** (2001) 117 [arXiv:hep-ph/0106189]; L. Roszkowski, R. Ruiz de Austri and T. Nihei, *JHEP* **0108** (2001) 024 [arXiv:hep-ph/0106334]; A. Djouadi, M. Drees and J. L. Kneur, *JHEP* **0108** (2001) 055 [arXiv:hep-ph/0107316]; U. Chattopadhyay, A. Corsetti and P. Nath, *Phys. Rev. D* **66** (2002) 035003 [arXiv:hep-ph/0201001]; J. R. Ellis, K. A. Olive and Y. Santoso, *New Jour. Phys.* **4** (2002) 32 [arXiv:hep-ph/0202110]; H. Baer, C. Balazs, A. Belyaev, J. K. Mizukoshi, X. Tata and Y. Wang, *JHEP* **0207** (2002) 050 [arXiv:hep-ph/0205325]; R. Arnowitt and B. Dutta, arXiv:hep-ph/0211417.
- [49] A. M. Sirunyan *et al.* [CMS], *Eur. Phys. J. C* **80** (2020) no.1, 3 [arXiv:1909.03460 [hep-ex]].
- [50] G. Aad *et al.* [ATLAS], *Phys. Rept.* **1116** (2025), 261-300 [arXiv:2403.02455 [hep-ex]].
- [51] E. Arganda, M. de los Rios, A. D. Perez, S. Roy, R. M. Sandá Seoane and C. E. M. Wagner,
- [52] P. Slavich, “Precision calculations in supersymmetric extensions of the Standard Model,” tel-00824019.
- [53] U. Ellwanger, J. Gunion, C. Hugonie, *JHEP* **02** (2005) 066 [arXiv:hep-ph/0406215].
- [54] U. Ellwanger, C. Hugonie, *Comput. Phys. Commun.* **175** (2006) 290, [arXiv:hep-ph/0508022].
- [55] F. Domingo, *JHEP* **06** (2015) 052, [arXiv:1503.07087 [hep-ph]].
- [56] See: <https://www.lupm.univ-montp2.fr/users/nmssm/>.
- [57] G. Degrandi and P. Slavich, *Nucl. Phys. B* **825** (2010), 119-150 [arXiv:0907.4682 [hep-ph]].
- [58] P. Slavich, S. Heinemeyer (eds.), E. Bagnaschi *et al.*, *Eur. Phys. J. C* **81** (2021) no.5, 450 [arXiv:2012.15629 [hep-ph]].
- [59] F. Domingo, S. Heinemeyer, S. Paßehr and G. Weiglein, *Eur. Phys. J. C* **78** (2018) no.11, 942 [arXiv:1807.06322 [hep-ph]].

- [60] K. Choi, S. H. Im, K. S. Jeong and C. B. Park, *Eur. Phys. J. C* **79** (2019) no.11, 956 [arXiv:1906.03389 [hep-ph]].
- [61] T. Biekötter, A. Grohsjean, S. Heinemeyer, C. Schwanenberger and G. Weiglein, *Eur. Phys. J. C* **82** (2022) no.2, 178 [arXiv:2109.01128 [hep-ph]].
- [62] K. Choi, S. H. Im, K. S. Jeong and C. B. Park, *Eur. Phys. J. C* **79** (2019) no.11, 956 [arXiv:1906.03389 [hep-ph]].
- [63] J. Cao, X. Jia, Y. Yue, H. Zhou and P. Zhu, *Phys. Rev. D* **101** (2020) no.5, 055008 [arXiv:1908.07206 [hep-ph]].
- [64] W. Li, H. Qiao and J. Zhu, *Chin. Phys. C* **47** (2023) no.12, 123102 [arXiv:2212.11739 [hep-ph]].
- [65] U. Ellwanger and C. Hugonie, *Eur. Phys. J. C* **83** (2023) no.12, 1138 [arXiv:2309.07838 [hep-ph]].
- [66] J. Cao, X. Jia and J. Lian, *Phys. Rev. D* **110** (2024) no.11, 115039 [arXiv:2402.15847 [hep-ph]].
- [67] U. Ellwanger and C. Hugonie, *Eur. Phys. J. C* **84** (2024) no.5, 526 [arXiv:2403.16884 [hep-ph]].
- [68] J. Lian, *Phys. Rev. D* **110** (2024) no.11, 115018 [arXiv:2406.10969 [hep-ph]].
- [69] T. Biekötter, S. Heinemeyer and C. Muñoz, *Eur. Phys. J. C* **78** (2018) no.6, 504 [arXiv:1712.07475 [hep-ph]].
- [70] T. Biekötter, S. Heinemeyer and C. Muñoz, *Eur. Phys. J. C* **79** (2019) no.8, 667 [arXiv:1906.06173 [hep-ph]].
- [71] W. G. Hollik, S. Liebler, G. Moortgat-Pick, S. Paßehr and G. Weiglein, *Eur. Phys. J. C* **79** (2019) no.1, 75 [arXiv:1809.07371 [hep-ph]].
- [72] G. Belanger, F. Boudjema, A. Pukhov and A. Semenov, *Comput. Phys. Commun.* **149** (2002), 103-120 [arXiv:hep-ph/0112278 [hep-ph]].
- [73] G. Belanger, F. Boudjema, A. Pukhov and A. Semenov, *Comput. Phys. Commun.* **176** (2007), 367-382 [arXiv:hep-ph/0607059 [hep-ph]].
- [74] G. Belanger, F. Boudjema, A. Pukhov and A. Semenov, *Comput. Phys. Commun.* **177** (2007), 894-895.
- [75] G. Belanger, F. Boudjema, A. Pukhov and A. Semenov, arXiv:1305.0237 [hep-ph].
- [76] G. Bélanger, F. Boudjema, A. Pukhov and A. Semenov, *Comput. Phys. Commun.* **192** (2015), 322-329 [arXiv:1407.6129 [hep-ph]].
- [77] D. Barducci, G. Belanger, J. Bernon, F. Boudjema, J. Da Silva, S. Kraml, U. Laa and A. Pukhov, *Comput. Phys. Commun.* **222** (2018), 327-338 [arXiv:1606.03834 [hep-ph]].

- [78] G. Bélanger, F. Boudjema, A. Goudelis, A. Pukhov and B. Zaldivar, *Comput. Phys. Commun.* **231** (2018), 173-186 [arXiv:1801.03509 [hep-ph]].
- [79] G. Belanger, A. Mjallal and A. Pukhov, *Eur. Phys. J. C* **81** (2021) no.3, 239 [arXiv:2003.08621 [hep-ph]].
- [80] G. Alguero, G. Belanger, F. Boudjema, S. Chakraborti, A. Goudelis, S. Kraml, A. Mjallal and A. Pukhov, *Comput. Phys. Commun.* **299** (2024), 109133 [arXiv:2312.14894 [hep-ph]].
- [81] Z. Bo *et al.* [PandaX], *Phys. Rev. Lett.* **134** (2025) no.1, 011805 [arXiv:2408.00664 [hep-ex]].
- [82] J. Aalbers *et al.* [LZ], *Phys. Rev. Lett.* **135** (2025) no.1, 011802 [arXiv:2410.17036 [hep-ex]].
- [83] E. Aprile *et al.* [XENON], *Phys. Rev. Lett.* **135** (2025) no.22, 221003 [arXiv:2502.18005 [hep-ex]].
- [84] T. R. Slatyer, arXiv:1710.05137 [hep-ph].
- [85] A. Hryczuk, K. Jodlowski, E. Moulin, L. Rinchuso, L. Roszkowski, E. M. Sessolo and S. Trojanowski, *JHEP* **10** (2019), 043 [arXiv:1905.00315 [hep-ph]].
- [86] L. Rinchuso, O. Macias, E. Moulin, N. L. Rodd and T. R. Slatyer, *Phys. Rev. D* **103** (2021) no.2, 023011 [arXiv:2008.00692 [astro-ph.HE]].
- [87] R. T. Co, B. Sheff and J. D. Wells, *Phys. Rev. D* **105** (2022) no.3, 035012 [arXiv:2105.12142 [hep-ph]].
- [88] A. McDaniel, M. Ajello, C. M. Karwin, M. Di Mauro, A. Drlica-Wagner and M. Sánchez-Conde, arXiv:2311.04982 [astro-ph.HE].
- [89] M. Ackermann *et al.* [Fermi-LAT], *Phys. Rev. Lett.* **115** (2015) no.23, 231301 [arXiv:1503.02641 [astro-ph.HE]].
- [90] P. Bechtel, S. Heinemeyer, O. Stål, T. Stefaniak and G. Weiglein, *Eur. Phys. J. C* **74** (2014) no.2, 2711 [arXiv:1305.1933 [hep-ph]].
- [91] P. Bechtel, S. Heinemeyer, O. Stål, T. Stefaniak and G. Weiglein, *JHEP* **1411** (2014) 039 [arXiv:1403.1582 [hep-ph]].
- [92] P. Bechtel, S. Heinemeyer, T. Klingl, T. Stefaniak, G. Weiglein and J. Wittbrodt, *Eur. Phys. J. C* **81** (2021) no.2, 145 [arXiv:2012.09197 [hep-ph]].
- [93] H. Bahl, T. Biekötter, S. Heinemeyer, C. Li, S. Paasch, G. Weiglein and J. Wittbrodt, *Comput. Phys. Commun.* **291** (2023), 108803 [arXiv:2210.09332 [hep-ph]].
- [94] H. Bahl, T. Biekötter, S. Heinemeyer, K. Radchenko and G. Weiglein, IFT-UAM/CSIC-25-072 (to appear).

- [95] P. Bechtle, O. Brein, S. Heinemeyer, G. Weiglein and K. E. Williams, *Comput. Phys. Commun.* **181** (2010) 138 [arXiv:0811.4169 [hep-ph]].
- [96] P. Bechtle, O. Brein, S. Heinemeyer, G. Weiglein and K. E. Williams, *Comput. Phys. Commun.* **182** (2011) 2605 [arXiv:1102.1898 [hep-ph]].
- [97] P. Bechtle, O. Brein, S. Heinemeyer, O. Stål, T. Stefaniak, G. Weiglein and K. E. Williams, *Eur. Phys. J. C* **74** (2014) no.3, 2693 [arXiv:1311.0055 [hep-ph]].
- [98] P. Bechtle, S. Heinemeyer, O. Stål, T. Stefaniak and G. Weiglein, *Eur. Phys. J. C* **75** (2015) no.9, 421 [arXiv:1507.06706 [hep-ph]].
- [99] P. Bechtle, D. Dercks, S. Heinemeyer, T. Klingl, T. Stefaniak, G. Weiglein and J. Wittbrodt, *Eur. Phys. J. C* **80** (2020) no.12, 1211 [arXiv:2006.06007 [hep-ph]].
- [100] T. Enomoto and R. Watanabe, *JHEP* **1605** (2016) 002 [arXiv:1511.05066 [hep-ph]].
- [101] A. Arbey, F. Mahmoudi, O. Stål and T. Stefaniak, *Eur. Phys. J. C* **78** (2018) no.3, 182 [arXiv:1706.07414 [hep-ph]].
- [102] M. M. Altakach, S. Kraml, A. Lessa, S. Narasimha, T. Pascal, C. Ramos, Y. Villamizar and W. Waltenberger, *JHEP* **11**, 074 (2024) [arXiv:2409.12942 [hep-ph]].
- [103] S. Kraml, S. Kulkarni, U. Laa, A. Lessa, W. Magerl, D. Proschofsky-Spindler and W. Waltenberger, *Eur. Phys. J. C* **74**, 2868 (2014) [arXiv:1312.4175 [hep-ph]].
- [104] F. Ambrogio *et al.*, *Comput. Phys. Commun.* **251**, 106848 (2020) [arXiv:1811.10624 [hep-ph]].
- [105] G. Alguero, S. Kraml and W. Waltenberger, *Comput. Phys. Commun.* **264**, 107909 (2021) [arXiv:2009.01809 [hep-ph]].
- [106] G. Alguero, *et al.*, *JHEP* **08**, 068 (2022) [arXiv:2112.00769 [hep-ph]].
- [107] A. Djouadi, J. Kalinowski and M. Spira, *Comput. Phys. Commun.* **108** (1998), 56-74 [arXiv:hep-ph/9704448 [hep-ph]].
- [108] A. Djouadi *et al.* [HDECAY], *Comput. Phys. Commun.* **238** (2019), 214-231 [arXiv:1801.09506 [hep-ph]].
- [109] M. Mühlleitner, A. Djouadi and Y. Mambrini, *Comput. Phys. Commun.* **168** (2005) 46 [hep-ph/0311167].
- [110] F. Feroz, M. P. Hobson and M. Bridges, *Mon. Not. Roy. Astron. Soc.* **398** (2009), 1601-1614 [arXiv:0809.3437 [astro-ph]].
- [111] P. Z. Skands, *et al.*, *JHEP* **07** (2004), 036 [arXiv:hep-ph/0311123 [hep-ph]].
- [112] B. C. Allanach, *et al.*, *Comput. Phys. Commun.* **180** (2009), 8-25 [arXiv:0801.0045 [hep-ph]].

- [113] J. Alwall, R. Frederix, S. Frixione, V. Hirschi, F. Maltoni, O. Mattelaer, H. S. Shao, T. Stelzer, P. Torrielli and M. Zaro, *JHEP* **07**, (2014) 079 [arXiv:1405.0301 [hep-ph]].
- [114] A. Alloul, N. D. Christensen, C. Degrande, C. Duhr and B. Fuks, *Comput. Phys. Commun.* **185**, (2014) 2250-2300 [arXiv:1310.1921 [hep-ph]].
- [115] E. Conte, B. Fuks, J. Guo, J. Li and A. G. Williams, *JHEP* **05**, (2016) 100 [arXiv:1604.05394 [hep-ph]].
- [116] B. Fuks, M. Klasen, D. R. Lamprea and M. Rothering, *Eur. Phys. J. C* **73** (2013), 2480 [arXiv:1304.0790 [hep-ph]].
- [117] G. Bozzi, B. Fuks and M. Klasen, *Phys. Rev. D* **74** (2006), 015001 [arXiv:hep-ph/0603074 [hep-ph]].
- [118] G. Bozzi, B. Fuks and M. Klasen, *Nucl. Phys. B* **777** (2007), 157-181 [arXiv:hep-ph/0701202 [hep-ph]].
- [119] J. Debove, B. Fuks and M. Klasen, *Phys. Lett. B* **688** (2010), 208-211 [arXiv:0907.1105 [hep-ph]].
- [120] J. Debove, B. Fuks and M. Klasen, *Nucl. Phys. B* **842** (2011), 51-85 [arXiv:1005.2909 [hep-ph]].
- [121] G. Degrassi, S. Heinemeyer, W. Hollik, P. Slavich and G. Weiglein, *Eur. Phys. J. C* **28** (2003), 133-143 [arXiv:hep-ph/0212020 [hep-ph]].
- [122] C. E. Aalseth *et al.* [DarkSide-20k], *Eur. Phys. J. Plus* **133** (2018), 131 [arXiv:1707.08145 [physics.ins-det]].
- [123] J. Aalbers *et al.* [XLZD], *Eur. Phys. J. C* **85** (2025) no.10, 1192 [arXiv:2410.17137 [hep-ex]].
- [124] J. Billard, L. Strigari and E. Figueroa-Feliciano, *Phys. Rev. D* **89** (2014) no.2, 023524 [arXiv:1307.5458 [hep-ph]].
- [125] F. Ruppin, J. Billard, E. Figueroa-Feliciano and L. Strigari, *Phys. Rev. D* **90** (2014) no.8, 083510 [arXiv:1408.3581 [hep-ph]].
- [126] P. N. Bhattiprolu, S. P. Martin and J. D. Wells, [arXiv:2512.12457 [hep-ph]].
- [127] C. Amole *et al.* [PICO], *Phys. Rev. D* **100** (2019) no.2, 022001 [arXiv:1902.04031 [astro-ph.CO]].